THESIS FOR THE DEGREE OF DOCTOR OF PHILOSOPHY IN THERMO AND FLUID
DYNAMICS

Predictive model of perceived driving stability at high speeds under aerodynamic excitations

ARUN KUMAR

Department of Mechanics and Maritime Sciences

CHALMERS UNIVERSITY OF TECHNOLOGY

Göteborg, Sweden 2023

Predictive model of perceived driving stability at high speeds under aerodynamic excitations
ARUN KUMAR
ISBN 978-91-7905-870-8

Predictive model of perceived driving stability at high speeds under aerodynamic excitations
ARUN KUMAR
Department of Mechanics and Maritime Sciences
Chalmers University of Technology

Abstract

The automotive industry is continuously advancing towards more energy-efficient vehicle designs. Streamlined vehicles have low aerodynamic drag but have the potential to be unstable when exposed to external excitations such as unsteady aerodynamic forces created by the flow of air around them. Before signing off a new vehicle for production, several on-road test scenarios are conducted by professional drivers to evaluate the performance. Finding vehicle instabilities and proposing solutions to problems during late phases of development is challenging and costly. The objective of this thesis is to correlate and predict the driver's subjective evaluation of high speed straight-line driving stability with measurable quantities in early design phases.

In this work, substandard straight-line drivability was investigated on-road using different aerodynamic devices for generating high rear lift and asymmetric aerodynamic forces. These aerodynamic devices were then paired with stabilizers, called side-kicks, which helped to define the flow separation and improved the drivability of the tested vehicle. Vector plots of the mean and standard deviation of lateral acceleration, yaw velocity, steering angle, and steering torque were used to understand vehicle behaviour for the paired configurations and relate to the difference of subjective evaluation of drivability within each pair. The ride diagram was used to separate the presence of transient behaviour and study its impact on subjective evaluation. The qualitative assessment of the resulting trends agreed well with the subjective evaluation of the driver.

Following this, experimental trials were conducted in driving simulators and on-road, in order to have an in-depth understanding of drivers' subjective evaluation and responses to external excitations. Both common and professional test drivers were involved in the study. The results provided insight into the excitation frequencies and amplitudes of interest. From the test data, mathematical models were generated that can predict the drivers' subjective evaluation after experiencing induced external excitations. The outcome showed the impact of drivers' steering on their subjective evaluations towards these excitations. The on-road study revealed that higher roll and longitudinal noises reduce the drivers' sensitivity to external excitations. Headwind magnitude and lateral motion in a certain frequency range experienced by the human upper body contribute to drivers' identification of excitations. The resulting predictive model can be used to pinpoint the time of occurrence of observable aerodynamic excitations and provides their characteristics in early development phases. Since the models represent measurements from the cabin, they should be valid for different vehicles.

Keywords: Driving simulator, on-road tests, driver-vehicle interaction, unsteady aerodynamics, vehicle stability, predictive model, subjective evaluation.

"Strong people don't put others down. They lift them up." —Darth Vader, Philanthropist

Acknowledgements

Arun Kumar
Göteborg, June 2023

<center>Nomenclature</center>

Abbreviations

CAN	Controller Area Network
CFD	Computational Fluid Dynamics
DOF	Degree of Freedom
FFT	Fast Fourier transform
IMU	Inertia Measurement Unit
MCA	Motion Cueing Algorithm
MS	Mean Squared Value
OEM	Original Equipment Manufacturer
RMS	Root Mean Square Value
SUV	Sports Utility Vehicle
VTI	Statens Väg- och Transportforskninginstitut (Swedish National Road and Transport Research Institute)

Symbols

$\bar{H}_{\delta_{sw}\to\omega_i}$	Weighted transfer function for steering input to rotational rate	[-]
$\bar{H}_{\delta_{sw}\to a_y}$	Weighted transfer function for steering input to lateral acceleration	[-]
$\delta_{front\,axis}$	Front wheel angle	[deg]
δ_{sw}, δ_{SW}	Steering wheel angle	[deg]
$\dot{\delta}_{sw}$	Steering rate	[deg/s]
$\dot{\omega}_x$	Roll acceleration	[deg/s^2]
$\dot{\omega}_z$	Yaw acceleration	[deg/s^2]
$\dot{\phi}_{vh}, \omega_x$	Roll velocity	[deg/s]
$\dot{\psi}_{vh}, \omega_z$	Yaw velocity	[deg/s]
$\dot{\theta}_{vh}, \omega_y$	Pitch velocity	[deg/s]
ω_i^{excess}	Excess rotational rate	[deg/s]
ω_i^{steer}	Rotational rate caused by steering	[deg/s]
ω_x^{excess}	Excess roll velocity	[deg/s]
ω_x^{steer}	Roll velocity caused by steering	[deg/s]
ω_z^{excess}	Excess yaw velocity	[deg/s]
ω_z^{steer}	Yaw velocity caused by steering	[deg/s]
ϕ_{vh}	Roll angle	[deg]
ψ_{vh}	Yaw angle	[deg]

τ_{sw}	Steering wheel torque	[Nm]
θ_{vh}	Pitch angle	[deg]
$\vec{\omega}$	Vehicle body angular velocity vector	[deg/s]
$\vec{a}$	Vehicle body acceleration vector	[m/s^2]
ζ	Look-ahead time	[s]
a_x, $\ddot{x}_{vh}$	Longitudinal acceleration	[m/s^2]
a_y, $\ddot{y}_{vh}$	Lateral acceleration	[m/s^2]
a_y^{excess}	Excess lateral acceleration	[m/s^2]
a_y^{steer}	Lateral acceleration caused by steering	[m/s^2]
a_z, $\ddot{z}_{vh}$	Vertical acceleration	[m/s^2]
$a_{y,head}$	Lateral acceleration measured at headrest	[m/s^2]
c_{DT}	Driver type	[-]
C_{lf}	Aerodynamic coefficient of front lift force	[-]
C_{lr}	Aerodynamic coefficient of rear lift force	[-]
$H_{\delta_{sw} \to \omega_i}$	Transfer function for steering input to rotational rate	[-]
M_z	Yaw moment	[Nm]
s, t	Time	[s]
v_x	Vehicle longitudinal velocity	[m/s]
$v_{wind,mag}$	Absolute headwind magnitude	[m/s]
y_{vh}	Lateral displacement	[m]

Definitions

$p2p$	Peak-to-peak value
std	Standard deviation
High Speed	$\geq$ 200 km/h

THESIS

This thesis consists of an extended summary and the following appended papers:

Paper A Kumar, A., Sebben, S., Sällström, E., Jacobson, B. J. H., and Broniewicz, A. "Analysis of Subjective Qualitative Judgement of Passenger Vehicle High Speed Drivability due to Aerodynamics". *Energies* **12**.14 (2019). DOI: 10.3390/en12142839

Paper B Kumar, A., Sällström, E., Sebben, S., Amiri, K., and Jacobson, B. "Prediction of Driver's Subjective Perception and Vehicle Reaction under Aerodynamic Excitations". *Human Factors* (2023). DOI: 10.1177/00187208231157935

Paper C Kumar, A., Sällström, E., Sebben, S., and Jacobson, B. "Improved Prediction Model of Drivers' Subjective Perception of Vehicle Reaction under Aerodynamic Excitations". *To be submitted* (2023)

Paper D Kumar, A., Sällström, E., Sebben, S., and Jacobson, B. "Predictive Model of Driver's Perception of Vehicle Stability under Aerodynamic Excitation". *SAE Technical Paper Series* (2023). DOI: 10.4271/2023-01-0903

Division of work

- Paper A: All instrumentation setup, data acquisition, and analysis were done by Kumar. The high speed driving at the test track was performed by Kumar with the support of three experienced test drivers from Volvo Cars. The first manuscript was written by Kumar then discussed, reviewed, and revised by all authors.
- Paper B and C: All instrumentation setup, data acquisition, and analysis were done by Kumar. The driving simulator setup was done by Kumar with dedicated people at Volvo Cars' driving simulator and VTI. The high speed driving in the driving simulator was performed by engineers at Volvo Cars and PhD colleagues. Kumar together with Sällström build the predictive regression model. The first manuscript was written by Kumar then discussed, reviewed, and revised by all authors.
- Paper D: All instrumentation setup, data acquisition, and analysis were done by Kumar. The high speed driving at the test track was performed by Kumar with the support of experienced test drivers/engineers at Volvo Cars. Kumar together with Sällström build the predictive regression model. The first manuscript was written by Kumar then discussed, reviewed, and revised by all authors.

Contents

Part I

Extended summary

1

Introduction

This thesis brings insight into passenger vehicle driving stability in high speed straight-line cruising conditions. It focuses mainly on relating the subjective evaluation of drivers to physically computable and measurable quantities such as linear and rotational motions, and steering characteristics. Subjective evaluation, vehicle dynamics, and aerodynamics are the key fields coupled in this study.

Designing a vehicle is challenging as it needs to impress the customer both aesthetically and with energy efficiency. The impact of aerodynamic drag is becoming increasingly in focus, especially with the electrification of vehicles due to its implication on the drive range. Designing a vehicle with low aerodynamic drag might bring in susceptibility to vehicle instabilities. Pre-production vehicles are tested on-road by professional test drivers to subjectively assess the driving dynamics and vehicle stability in different driving scenarios. These tests take place in the later phase of development. The test drivers usually rate the vehicle's performance for high speed cornering, high speed lane maneuvers, high speed braking, vehicle response to gusts, etc. For the assurance of safety and vehicle performance quality, these tests are conducted up to the maximum potential of the vehicle. In this study, straight-line driving at constant high speeds of 200 km/h and higher is the scenario in focus.

Nervousness, termed by test drivers, is a vehicle instability behaviour felt while driving in a straight line. The causes of nervousness can be many but the one in focus in this study results from vehicle instabilities induced by unsteady aerodynamic forces. Unsteady aerodynamics constantly influences vehicle performance and increasingly so at high speeds. For drivers, such nervousness can produce subjective impressions ranging from merely inconvenient to alarmingly unacceptable behaviour of the vehicle. Finding such impressions during on-road tests is not desirable by OEM. In this work, several studies are conducted to find ways to improve the prediction of such subjective evaluations from test drivers and relate those to objective measurable quantities in the early stage of vehicle development. From the test data, mathematical models are generated that can predict the drivers' subjective evaluation after experiencing induced external excitations.

1.1   Background

The stability of a vehicle is determined by a combination of aerodynamics, vehicle dynamics, driver, and environment. The vehicle and driver's response to the influence of external disturbances provides an understanding of the vehicle's stability. In this study, the focus is on

the subjective evaluation of vehicles under high speed straight-line cruise driving. The high speed in this thesis refers to speeds 200 km/h and higher.

The background on the relation between the subjective evaluation of vehicle stability is described in this chapter. Related on-road and driving simulator studies and the basic working principle of the driving simulator are explained. Thereafter, a brief overview of subjective perception is discussed.

1.1.1 Evaluation of vehicle stability

There are different approaches to evaluating if a vehicle design is aerodynamically stable. One common approach that is straightforward and simple is by using only aerodynamic forces and moments as measured variables of stability in conditions such as crosswinds and improves the stability of the vehicle through minimized yaw moments and total lift and side forces. Aerodynamic coefficients for yaw and lift are a function of the vehicle shape and initial aerodynamic design studies use this stability reference for development [1]. This is often practiced in the automotive industry. Although simple, this criteria might not be sufficient, as demonstrated by Brandt, A. [2].

Another approach is with one-way or two-way coupling of aerodynamics and vehicle dynamics. Some studies run aerodynamic simulations separately and then feed the aerodynamic data to a vehicle dynamic model, termed one-way coupling [3–5]. Other studies investigate the effective vehicle orientation to disturbances and the resulting effect on flow conditions through concurrent aerodynamic and vehicle dynamic simulations [6–11]. This is termed two-way coupling. Some studies have investigated the aerodynamic response approach where the effective transient aerodynamic load from gusty wind conditions is estimated from inverse simulations of dynamic models of the vehicle [12–14]. This approach makes it possible to study the aerodynamic loads without a full-scale wind tunnel adapted for crosswind excitation. The vehicle dynamic response approach was studied using a vehicle dynamics model of varying degrees of complexity coupled with aerodynamic loads under a given aerodynamic condition [3, 9, 10].

Even vehicle setups configured to be stable through the aforementioned approaches can turn out to be subjectively evaluated as unstable by drivers. Therefore, aerodynamic-vehicle dynamic coupling simulations should benefit from being further extended with the implementation of a driver model, for example, as done in [2, 12, 15]. The addition helps the development of a more realistic vehicle response by including a driver's input. However, such models can be prone to the uncertainty of a real driver's behaviour following external excitations. Currently, the study of drivers' subjective evaluation of vehicle stability is best investigated through on-road and driving simulator testing. The background on these methods is explained in the succeeding subsections.

On-road test

On-road tests are used by automobile manufacturers in the last phase of development for the final tuning and evaluation of vehicle performance. On-road tests simulate more realistic driving conditions, the drivers are more involved and do not have the false sense of safety as in a driving simulator. This experience results in responses that are more realistic. On the other

hand, the external environment is neither controllable nor repeatable. A lot more testing is required for achieving statistical significance when implementing a standardized driving test under potentially high random noise. Typically, it is not realistic to do as much testing as is desired due to cost, time, and resource constraints. Moreover, certain on-road maneuvers might be hazardous and ethically inappropriate.

The aerodynamics affecting vehicle stability can be due to external excitations such as impacts of wind gusts, a consequence of vehicle motion due to road unevenness [16–21], or as a result of induced complex flow structures due to the shape of the vehicle, as studied in [22–24]. Okada et al. [22] used on-road and wind tunnel tests to show the influence of rear lift fluctuations and the A-pillar vortices on vehicle stability. Kawakami et al. [24] improved vehicle performance by reducing the aerodynamic load fluctuations on a hatchback with the help of vortex generators. The study was done using CFD and scale model wind tunnel experiments, followed by on-road tests. The preliminary study, using CFD and wind tunnel, showed how vortex generators suppressed the aerodynamic yaw and roll moment fluctuations by creating a more distinct flow separation region. They proved to improve the subjective rating during on-road tests.

Howell and Le Good [25] investigated the influence of front axle lift coefficient C_{lf} and rear axle lift coefficient C_{lr} on straight-line and lane change stability for several kinds of passenger vehicles. The lift coefficients were obtained from wind tunnel tests. The results provided initial design criteria of $C_{lf} + C_{lr} \leq 0.2$ and $|C_{lf} - C_{lr}| \leq 0.1$ for a stable vehicle. Buchheim et al. [26] investigated the influence of aerodynamic parameters on vehicle stability under high speed straight-line, braking, and crosswind conditions. Results from their on-road tests provide insight into preliminary stability criteria. Low overall lift force with a positive pitching moment is desirable for good vehicle dynamic performance under high speed straight-line driving scenarios. An increased rear lift in an exaggerated way demonstrates that the vehicle becomes unstable. Their work was the inspiration behind the modifications made to the rear of the vehicle on the first track tests performed in this study. Aerodynamic devices were added to increase the rear lift forces and consequently, decrease tire grip. Through reduced rear lateral grip between tires and road surfaces, the quality of vehicle straight-line stability was reduced.

Studies contributing to how on-road subjective vehicle nervousness correlates with measurable quantities such as acceleration, rotation or steering during straight-line driving are limited. Kim et al. [27] used deep neural networks to find an objective measure from subjective evaluation for various suspension settings. The trained network was capable of comparing the performance between models but did not give an assessment on absolute scale. A work by Wang et al. [28] focused on creating objective measures from subjective scores of ride comfort in autonomous driving under different on-road conditions such as acceleration around city traffic. Apfelbeck et al. [29] investigated a methodology to predict subjective impressions of ride quality under induced steering torque.

All these studies focused on ride quality and did not include high speed stability analysis. No methodology found by the author could pinpoint the time at which the aerodynamic excitations observed by the driver occurs in a transient condition. Such a methodology is useful to early identify the characteristics of aerodynamic excitations that can cause vehicle instability or a sense of nervousness by the driver.

Driving simulator test

Virtual simulation of on-road driving scenarios can be conducted using driving simulators with good repeatability as the environment is controlled. Current computational power can incorporate the full vehicle characteristics to conduct maneuvers such as high speed stability, crosswind, and primary ride (low-frequency high amplitude disturbances), already in early vehicle development. Analysis from such early tests can lead to sooner design decision making, resulting in better product performance and reduced development costs through fewer prototypes [30].

In a driving simulator, a realistic driving impression plays a significant role in the driver to absorb the virtual reality [31]. In order to enable simulations with the physical constraints of the simulator, most importantly the limited actuator stroke lengths, a motion cueing algorithm is used. A motion cueing algorithm (MCA) balances the actuated degrees of freedom (DOFs) according to the type of experiment and expectations within the physical constraints.

Motion platform

The driving simulators operated in this thesis use the hexapod system, which is a very commonly used hardware platform. It consists of six independently controlled prismatic actuators with the ability to transfer the load within 6 DOFs. These are:

Linear motion

- Surge: Translation along x axis
- Sway: Translation along y axis
- Heave: Translation along z axis

Rotation motion

- Roll: Turning around x axis
- Pitch: Turning around y axis
- Yaw: Turning around z axis

The hexapod system has limited stroke lengths and all DOFs are mechanically connected. As a result, the use of one DOF limits the stroke potential of the others. In the driving simulator used in this study, the whole platform is combined with an XY-sled which increases the stroke lengths further along the XY plane, shown in Figure 1.1. The simulator in this figure is used for the final clinical test, details of which are in [32–34].

Driving cues

Certain cues play a key role in perceived realism when simulating an on-road maneuver. They are:

- Visual cue: The computing delays between the computed position and direction of driver's view to visual display for the driver of the resulting motion in the simulator should be minimal. The visual latency of the simulator used for this study lied within 120 to 130 ms. According to Blissing et al. [35] the maximum thresholds for visual latency ranges

Figure 1.1: *VTI SimIV (Photo: Hejdlösa Bilder AB) [34]*

from 50 to 150 ms. Exceeding this threshold showed effects on driver's behaviour such as lane keeping and steering wheel reversal. Motion sickness and stress were other effects found at higher visual latency. The positioning of the observer in the platform should also be accurate enough to represent the desired visual sensation. The effect should also be minimal in this study due to less demanding maneuver.

- Steering torque feedback: The driver's haptic feedback is important. The steering wheel feedback provides the driver with an understanding of coupled interactions between the front axle tires and the road.

- Motion cueing algorithm: Vehicle motion is mapped to stay within the constraints of the driving simulator platform with the aim to create an experience as close to reality as possible for the human kinaesthetic sense and vestibular system. A motion cue algorithm maps the simulated vehicle motions to simulator motions. The classical motion cueing algorithm uses a frequency split approach as shown in Figure 1.2. The typical acceleration (or velocity) inputs from the simulated vehicle dynamics model to motion algorithm are:

    - linear accelerations: longitudinal $\ddot{x}_{vh}$, lateral $\ddot{y}_{vh}$ and vertical $\ddot{z}_{vh}$
    - rotational velocity: roll $\dot{\phi}_{vh}$, pitch $\dot{\theta}_{vh}$, yaw $\dot{\psi}_{vh}$

The obtained accelerations (or velocities) are distributed to the hexapod and sled systems based on the frequency range. The linear accelerations are divided between translation motion and tilt coordination. The sled system takes the middle frequency linear accelerations and the hexapod takes the high frequency linear accelerations. Low frequency linear accelerations are achieved by tilt coordination. Hexapod rotations will take this responsibility along with rotational velocity.

Several studies have assessed a driver's reaction to external disturbances using driving simulators, for example, Krantz et al. [36] who investigated the crosswind influence on vehicle dynamics.
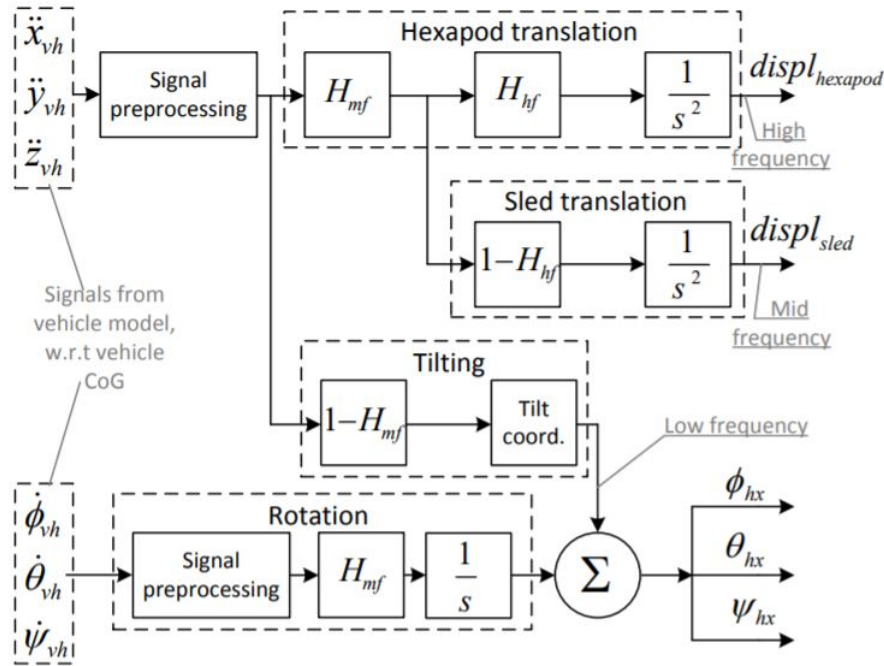
Figure 1.2: *Scheme of motion cue algorithm. Courtesy of A. Kusachov [33]*

The unsteady aerodynamic coefficients relating to the crosswind behavior of two different vehicles from wind tunnel tests were added to a single-track model. The drivers were asked to keep the vehicle in a straight-line. The investigated crosswind had a transient profile with a power spectral density peaking around 2 Hz. The results were used to study and compare the yaw and lateral response with those of on-road tests. The comparison showed a shift of the maximum yaw velocity towards lower frequencies in the driving simulator partly due to the effect of latencies on drivers' steering behaviour. Nevertheless, regarding variation in vehicle properties, the results reflected similarity to on-road tests, providing an insight into the application of driving simulators in unsteady aerodynamics in early development phase.

Huemer et al. [37] presented the influence of multidimensional vehicle response due to crosswind on driver perception also using a driving simulator. In their work, the multidimensional vehicle response consisted of roll velocity, yaw velocity, and lateral acceleration. The impact of amplitude changes of crosswinds and time delays between the resulting aerodynamic loads on the vehicle response was investigated. Yaw moment disturbance showed the highest influence on driving stability, subsequently side force, and roll moment. It was observed that the driver's perception of vehicle motion around the perception threshold was affected mainly by the lateral acceleration, yaw velocity, and time lag between them.

Nguyen et al. [38] investigated a cornering scenario on the German autobahn replicated in the simulator with vertical disturbances simulating road unevenness and road bumps. The vehicle's body motion was subjectively evaluated and the results included a threshold of sensitivity between pitch, roll, and lateral disturbance impulses over varying road noise intensities. In addition, the paper studied the difference in subjective impression in the case of coupled yaw and roll motion with different phase delays and amplitudes. When roll motion was perceived first followed by yaw motion, the sense of insecurity over vehicle motion increased. On the other

hand, the driver most likely rated the vehicle motion unrealistic if the roll motion had a positive phase lag over the yaw motion. While an increase in roll-to-yaw motion amplitude resulted in discomfort, an increase in roll-to-yaw motion amplitude resulted in a feel of unsecured vehicle motion.

Fuller et al. [39] also supported the importance of the unsteadiness of lateral aerodynamics from unsteady gusts on the subjective rating of vehicle stability using a simplified vehicle model geometry. The vehicle handling to different sources of unsteady crosswind was observed. The experimental aerodynamic loads were used in a dynamic model with six DOF. The vehicle model was coupled with a simulated driver model derived using driver data from a driving simulator study subjected to a crosswind. Only aerodynamic yaw moments and lateral forces were implemented in the simulator. The study showed that the large-scale onset change of wind had the largest impact on vehicle handling and subjective results. Furthermore, the stability impact study of other flow unsteadiness such as hysteresis, instantaneous unsteadiness, and vehicle front-to-rear time delay was found to be relatively small.

Literature on building a regression model that can predict the probability of a driver identifying an induced disturbance with the help of the measured quantities such as vehicle and driver behaviours is limited. For building this model, the driving simulator provides the ability to control the environment and reduced the impact of external noises affecting drivers' sensitivity.

1.1.2 Subjective perception

The vestibular system in the human body is responsible for human's ability to detect acceleration and orientation. The threshold for linear acceleration detection in vertical (z-axis), longitudinal (x-axis) and lateral (y-axis) directions was investigated in [40] and it was found to be 0.154 m/s^2, 0.063 m/s^2 and 0.057 m/s^2, respectively. This means that the threshold for vertical movement is significantly higher than the threshold of movement in longitudinal and vertical directions. The study in [40] was done with a single sinusoid disturbance without involving visual or auditory inputs on the participants. Groen et al. [41] found the rotational perception threshold as 3 deg/s. But this study was based on self-motion with four selected frequencies and amplitudes where the participants were more like a passenger. Mesland et al. [42] showed a rotational threshold value of 0.5 deg/s. The study was conducted in dark without visual aid. The threshold levels vary depending on many factors such as the test environment, visual and auditory inputs, disturbance frequencies, repetition of the test and the task of the participant such as driving.

As mentioned earlier in this chapter, difficulty in keeping the vehicle in the lane because of the presence of undesired vehicle oscillations is an unacceptable vehicle dynamics behaviour. Such vehicle oscillations can be due to external excitations and result in frequent steering corrections. The threshold of unacceptable vehicle dynamics behaviour varies with the drivers' sensitivity to perceived stability. Perceived stability is regarded as a subjective acceptance of a driver to a vehicle's behaviour under an excitation. During the subjective evaluation of vehicle performance, drivers' reaction to such vehicle dynamic behaviour is important [36, 43]. The impact of driver-vehicle system interaction on the subjective evaluation of the vehicle's perceived stability is significant.

Wagner and Wiedemann [43] found differences in drivers' reactions and judgements on vehicle behaviour depending on crosswind conditions. In the frequency range 0.5 - 1.5 Hz the drivers' steering intensity was quite high and resulted in amplified vehicle response. At crosswind conditions less than 0.5 Hz the drivers were capable of correcting the vehicle, however, above 2 Hz the changes were too fast for the drivers to respond.

For crosswind conditions, it is seen that yaw velocity and lateral acceleration have a strong correlation with subjective perception on stability [2]. From the related literature discussed in the previous section, generalized characteristics regarding drivers' subjective perception can be drawn. The drivers are highly sensitive to yaw moment followed by lateral acceleration, the influence of crosswind on yaw motion was the most sensitive and sensitivity reduces with increased road unevenness. The variation phase delays and amplitude ratio between roll and yaw moments showed the shift of drivers' subjective impression between uncomfortable and unsafe vehicle motion.

Presence of abrupt motion in the induced disturbance was found to get more attention from the driver than periodic disturbances [44, 45]. This observation led to the introduction of ride diagrams for analysis of ride comfort [46, 47]. A similar approach to lateral motion and steering behaviour showed potential in visually relating the subjective evaluation of perceived stability and measurable quantities.

The tests in this thesis investigate a high speed straight-line driving condition, during which the impact of driver fatigue is crucial for subjective response and limits the suitable duration of each test session. Driver fatigue can be a state of deterioration of mental alertness, or the transient state between sleep and awake, or psychological and physiological behaviour which when left undisturbed results in poor driver response to a given task [48–50]. Awareness decreases and sleepiness increases with prolonged monotonous driving [51, 52]. The studies suggest the test trial duration be kept below 15 minutes to minimize the impact of driving fatigue.

1.2 Thesis outline

Chapter 1 describes the purpose behind this project, narrates the necessary background of studies related to vehicle stability and subjective perception. Chapter 2 shortly presents the main objectives, and the limitations faced during the various tests. Chapter 3 explains the mathematical models, test vehicles and vehicle setups, and experimental trial design. Chapter 4 summarizes the most relevant findings from the whole study. Chapter 5 provides some final conclusions and Chapter 6 suggests future investigations. Finally, Chapter 7 summarizes each of the four papers.

2

Thesis objective

2.1 Research questions

This research aims to study and contribute to answering the following main research questions and sub-questions:

1. *For high speed straight-line driving under aerodynamic excitations, how can objective quantities such as steering response, and linear and rotational accelerations be related to the subjective evaluation of drivers?*

   How does the driver's evaluation relate to the measured objective quantities? Can eventual differences in subjective evaluation between cases be explained with objective quantities?

   Approach: On-road and driving simulator tests.

   Related work: Papers A, B, C, D.

2. *Is it possible to predict a driver's ability to identify an induced disturbance in an early vehicle design phase?*

   Can a driver's ability to identify an induced disturbance be predicted with a mathematical model? How do common drivers and professional test drivers react to external disturbances? What quantities, amplitudes, and frequencies are influential in drivers' evaluation of stability?

   Approach: On-road and driving simulator tests.

   Related work: Papers B, C, D.

3. *How can a predictive model be used to identify instabilities before any drivable vehicle prototype is available?*

   Approach: On-road and driving simulator tests.

   Related work: Thesis, Section 4.5.

2.2 Limitations

This study is limited to straight line driving under small, but distinct aerodynamic excitations, as opposed to constant wind and constantly varying wind environment. The speeds considered

were: Paper A, 230 and 250 km/h and Papers B, C, and D 200 km/h. The influence of acoustic and visual stimuli on a driver's stability evaluation is not investigated in this study. Influence from advanced steering assist functions is also not included, only traditional boost-curve-assist.

In the first on-road test (Paper A), the test vehicle was a mid-size, front-wheel driven, and front-weight-biased sedan. The test was conducted using only one type of tire. For the driving simulator test (Papers B and C), the vehicle model was a compact sports utility vehicle (SUV). The components of the vehicle dynamics model used for the clinical test, such as tires and steering, were generic. Resources constraints limit the sample size, number of drivers, and the number of variations of disturbances that can be studied. This also limited the implementation of road noise in the simulator to only include the vertical component. The test vehicle for the final on-road test (Paper D) was a mid-size, all-wheel drive SUV. This test was also conducted using only one type of tire. Since the individual tests were conducted on a single type of vehicle and set of tires, more tests involving different vehicles and tires would be needed to prove the generality of the conclusions.

Furthermore, fatigue and mind saturation were also factors limiting the duration of the tests. As a result, the thesis does not claim to have a good predictive model to judge perceived stability with respect to the influence of driver's performance on the driving duration or other individual performance uncertainties. However, despite all these limitations, this thesis still provides good insights into a better understanding of perceived vehicle stability.

3

Methodology

This chapter presents the overview of the methodology used in this study. Mathematical models are needed for analyzing and representing drivers' perceived stability with objective quantities. So the first section starts by briefly explaining the mathematical models used. The final section describes the experimental designs conducted in both on-road and driving simulator tests.

3.1   Mathematical models

Vector plots, ride diagrams, and logistic regression are used to relate the objective quantities with the perceived vehicle stability. These are explained in the following sections. The excess motion variables are important in the predictive model. The term excess motion will be defined and described later in this section. Paper A uses vector plots and ride diagrams, and Papers B, C, and D use logistic regression and excess motion.

3.1.1   Vector plots

Vector plots are used as an objective indicator for perceived vehicle stability, where vector lines join one configuration, marked as the tail, with another with improved subjective evaluation, marked as the arrow. A group of vectors that trend toward the origin implies improved perceived stability. The mean value and standard deviation of relevant objective quantities such as steering torque or yaw velocity are used.

Mean value

The mean is calculated for a quantity x according to the equation:

$$\bar{x} = \frac{1}{N}\sum_{i=1}^{N} x_i \tag{3.1}$$

where N is the number of samples.

Standard deviation

The number of independent samples, m, of each signal, x, is found using the auto-correlation function [53]. This function calculates the correlation between x_i and x_{i+k}, where lag $k = 1, 2, 3, ...K$. According to Box et al. [54] the auto-correlation for lag k is

$$r_k = \frac{c_k}{c_0} \tag{3.2}$$

where c_0 is the sample variance of the time series.

$$c_k = \frac{1}{N} \sum_{i=1}^{N-k} (x_i - \bar{x})(x_{i+k} - \bar{x}). \tag{3.3}$$

where N is the total number of observations. The auto-correlation time, τ, is

$$\tau = 1 + 2 \sum_{k=1}^{K} r_k \tag{3.4}$$

The effective sample size is

$$m = \frac{N}{\tau}. \tag{3.5}$$

The variance of the signals are:

$$\sigma_x^2 = \frac{1}{N} \sum_{i=1}^{N} (x_i - \bar{x})^2 \tag{3.6}$$

The σ_x obtained represents the standard deviation. The mean uncertainty with a coverage factor of 2, which corresponds to a coverage probability of approximately 95%, is:

$$U_{\bar{x}} = 2 \frac{1}{\sqrt{m}} \sigma_x \tag{3.7}$$

The resulting value is used for vector plotting.

3.1.2 Ride diagram

The ride diagram is another objective indicator used to relate the potential influence of objective quantities of transient nature to perceived stability. The method for the ride diagram is done in three steps, defined by Strandemar et al. [46, 47]. First, the signal of measure quantity is divided into segments at the sign changes of the signal derivatives as shown in Equation 3.8.

$$\Omega = \{n \mid x(n-1) > x(n) < x(n+1) \ \text{ or } \ x(n-1) < x(n) > x(n+1)\} \tag{3.8}$$

Thus the kth segment will be expressed as:

$$y_k = \{x(n)\}_{n=n_k}^{n=n_{k+1}} \tag{3.9}$$

Where $k = 1, 2, ..., N_{k-1}$ and N_k is the total number of peaks. The peak-to-peak value of kth segment is:

$$Ptp(k) = |\max(y_k) - \min(y_k)| \tag{3.10}$$

Second, the segments are categorized as transient or stationary according to:

$$y_{trans}^k = \begin{cases} \{x(n)\}_{n_k}^{n_{k+1}} & Ptp(k) > T_{limit} \ \& \ Ptp(k-1) \leqslant T_{limit} \\ \{x(n)\}_{n_k+1}^{n_{k+1}} & Ptp(k) > T_{limit} \ \& \ Ptp(k-1) > T_{limit} \\ 0 & \text{otherwise} \end{cases} \tag{3.11}$$

where $Ptp(0) = 0, \ k = 1, 2, ..., N_k - 1$ and $N_k - 1$ is the number of segments.

Figure 3.1(a) shows an example of a random signal. As referred in Strandemar et al. [46], $T_{limit} = 2\sqrt{2}\,RMS(x)$ is the limit of transients also known as the signal's energy equivalent amplitude.

Third, the Mean Squared Values (MS) of transient and stationary (remaining) signals are related as shown by the two equations:

$$MS_{transient} = \frac{1}{N} \sum_{k}^{N_k-1} \sum_{n} |y_{trans}^k|^2 \tag{3.12}$$
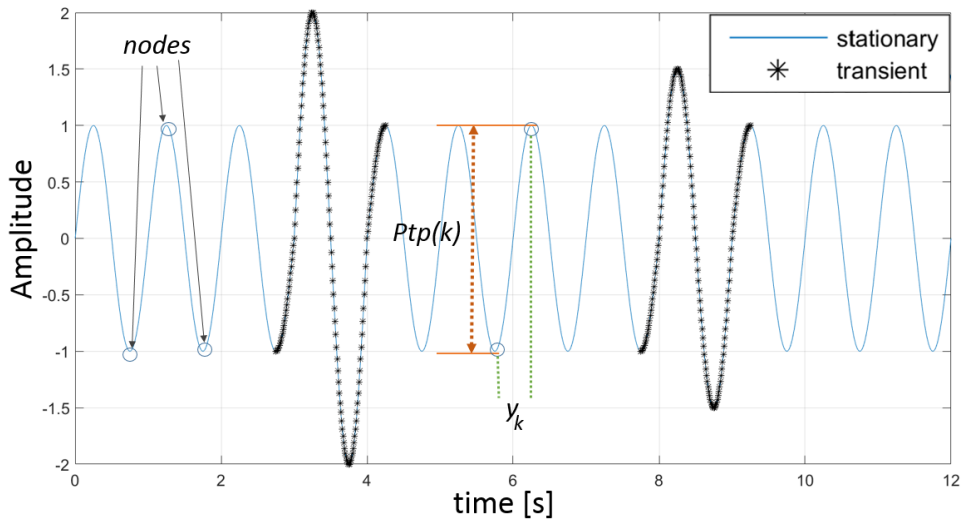
(a)
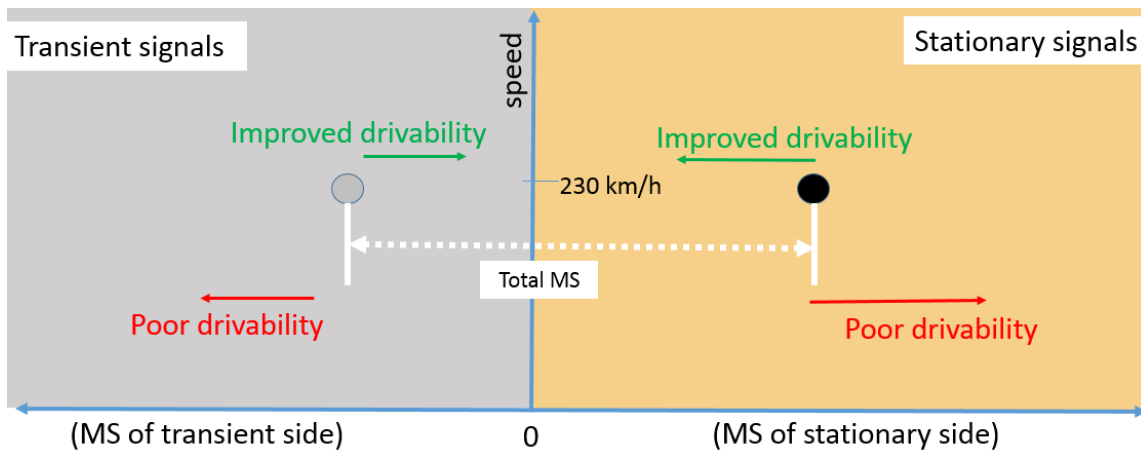
(b)

Figure 3.1: *Differentiation of stationary-transient signal derived from ride diagram of Strandemar [46]: (**a**) A signal divided into segments, where peak-to-peak, Ptp(k), distance is marked and the segments with asterisks are sorted as transient, and (**b**) A ride diagram, showing a simple representation of how to read the diagram. Left side represents Mean Squared Value (MS) of transient signals and right side represents Mean Squared Value (MS) of stationary signals.*
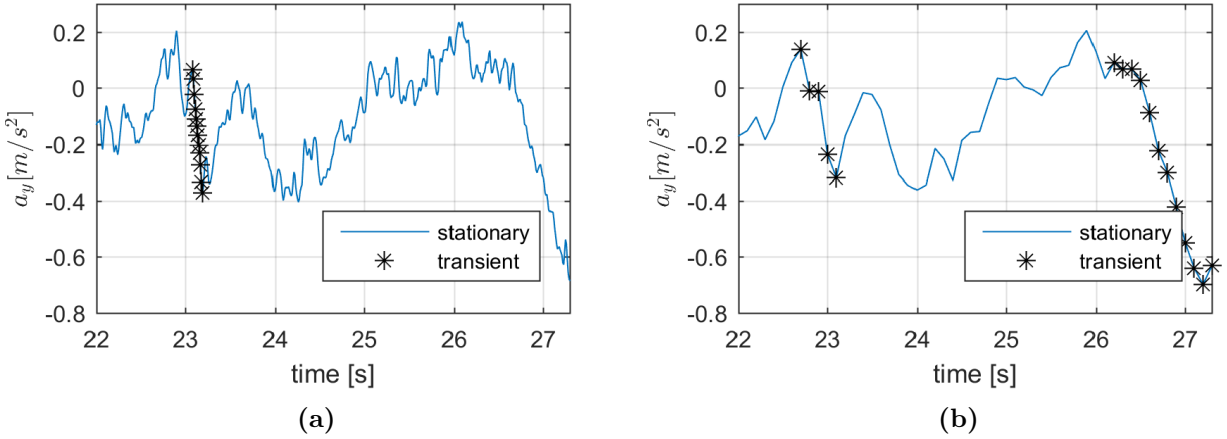
Figure 3.2: *Comparison of the ability to separate transient segments with different sample rates: (a) Lateral acceleration a_y vs time with a sample rate of 100 Hz, and (b) Lateral acceleration a_y vs time after downsampling to 10 Hz.*

$$MS_{stationary} = \frac{1}{N} \sum_{n=1}^{N} x(n)^2 - MS_{transient} \qquad (3.13)$$

For a given situation, Figure 3.1(b) shows the general idea of how to read the ride diagram with respect to perceived stability standards. The left side represents Mean Squared Value (MS) of transient signals and the right side represents Mean Squared Value (MS) of stationary signals. This method has some practical issues when the signals have small spikes. Spikes can be located in between an otherwise high peak-to-peak value as shown in Figure 3.2, from time 26 to 27 seconds. When separating the signals with the T_{limit} criterion, the algorithm only checks for the exact peak-to-peak values between these spikes. So the possibility is high for a peak-to-peak value, which would otherwise be eligible for being filtered as a transient segment, to not be filtered because of spikes. This can be reduced (but not eliminated) by downsampling the signals. The signal between 26 to 27 seconds is not considered transient in Figure 3.2(a) but it is considered transient in the downsampled signal shown in Figure 3.2(b) due to this reason. The method was originaly used by Strandemar for relatively simple signals for testing in a driving simulator. Hence, it needs further development for more realistic signals.

3.1.3   Logistic regression

Logistic regression is used here as a binomial classification technique, [55, 56]. It is used to predict the driver's subjective response from the governing measured vehicle and driver reactions. Consider the number of observations as n, R_i as the response, x_i as the independent variables called predictors, and k as the number of predictors. In this case, R_i consists of binary responses from the drivers (0 or 1). The objective of this approach is to create a response model that can predict the likelihood of each response R_i for given predictors on each observation.

Logistic regression is used to obtain the model coefficients needed to estimate the log-odds z of

the driver response being 1, in the linear function:

$$z \;=\; \beta_0 + \beta_1 x_1 + \beta_2 x_2 + ... + \beta_k x_k \tag{3.14}$$

where, β_0 is y-intercept and $\beta_{i=1,2,3..}$ are model coefficients of respective independent variables (predictors) $x_{i=1,2,3..}$.

A desired predictive model is established in the form of a logistic regression function $p(z) = 1/(1+\exp(-z))$. Where $p(z)$ is a sigmoid function and the value is the predicted probability of the response being 1 for a given observation. The logit model, $p(z)$, is a non-linear function. Finding the global minima while fitting model coefficients using the cost function further tunes the regression. This helps in selecting the best-suited predictors. Here, the MLE (maximum likelihood estimate) $= \sum_i (R_i \log(p(x_i)) + (1 - R_i)\log(1 - p(x_i)))$, is used. The resulting prediction accuracy can be classified as:

- Generic accuracy: The number of correct predictions over the total number of observations.
- True positive accuracy: The number of correctly predicted ones over the total number of observed ones.
- True negative accuracy: The number of correctly predicted zeros over the total number of observed zeros.

3.1.4 Excess motion

The cause for the motion in the cabin of a vehicle can be split into two parts. The first part is the result of steering if there is no other input. The second part is due to external inputs such as crosswinds or on-road inundations. An estimate of the latter is termed in this study as the excess motion.

The notations of variables shown here might vary from that of the papers presented in this study. The rotational velocities, denoted as ω_i, are measured from the cabin. The part of the rotational velocities that can be estimated from the steering is defined as ω_i^{steer}, and the rest is an approximation of the response to external disturbances, ω_i^{excess}.

$$\omega_i^{excess}(t) \;=\; \omega_i(t) - \omega_i^{steer}(t) \quad \text{where } i \in \{x, z\} \tag{3.15}$$

The ω_i^{steer} estimated from the steering angle, δ_{sw}, and longitudinal velocity, v_x, using the transfer function, $H_{\delta_{sw} \to \omega_i^{steer}}$. A direct transfer function from a sample window j is given by:

$$H_{\delta_{sw,j} \to \omega_{i,j}^{steer}}(f) \;=\; \frac{\mathcal{F}\{\omega_{i,j}^{steer}\}(f)}{\mathcal{F}\{v_x \cdot \delta_{sw,j}\}(f)} \tag{3.16}$$

For on-road tests, sample window j represent each drive of all drivers. For driving simulator tests, j represents each signal window of stimuli of all drivers.

In condition to the test scenarios in this study, the driving speed is kept as constant, $v_x = 200$ km/h, to minimize noise. A direct transfer function was not achieved because ω_i^{steer} is not a directly measured variable. Instead a transfer function, $H_{\delta_{sw,j} \to \omega_{i,j}}$, was achieved from Equation 3.16 by replacing ω_i^{steer} with the rotational rate, ω_i, logged from the cabin.

As a result, the transfer function used to estimate ω_i^{steer} from the steering angle, δ_{sw}, and longitudinal velocity, v_x, was taken from the weighted sum of all sample windows:

$$\bar{H}_{\delta_{sw}\to\omega_i^{steer}}(f) \;=\; \frac{\sum_j H_{\delta_{sw,j}\to\omega_{i,j}}(f)\cdot r_j}{\sum_j r_j} \tag{3.17}$$

Where r_j is a weighting factor for each sample window, j. The weighted approach of each transfer function, derived once per drive from all drives along straight lines parts of the test track, minimizes the influence of transient external excitations.

In the analysis of the driving simulator data, only time segments without any added disturbance in each j were used to calculate the transfer function. The *Before Disturbance* time segments were used, further explained in second half of Section 3.2.3. As a result, the weighted transfer function, $\bar{H}_{\delta_{sw}\to\omega_i^{steer}}$, approximately projects the steering-vehicle dynamics system characteristics and $\omega_{i,j}^{steer}$ is determined from $\delta_{sw,j}$ using this weighted transfer function.

Through the positive real part of the inverse Fourier transform of the weighted transfer function, $Re(\mathcal{F}^{-1}\{\bar{H}_{\delta_{sw}\to\omega_i^{steer}}\})$, the predicted rotational rate due to steering, ω_i^{steer}, from all sample windows along straights lines is obtained in time domain using convolution, denoted by $*$.

$$\omega_i^{steer}(t) \;=\; Re(\mathcal{F}^{-1}\{\bar{H}_{\delta_{sw}\to\omega_i^{steer}}\}) * (\delta_{sw}\cdot v_x)(t) \tag{3.18}$$

The excess rotational velocities due to external excitations, ω_i^{excess}, are obtained from Equation 3.15. A similar approach is followed for linear motion. In the case of excess lateral acceleration, a_y^{excess}, the weighted transfer function, $\bar{H}_{\delta_{sw}\to a_y^{steer}}$, is obtained from the product of steering angle, δ_{sw}, and squared longitudinal velocity, v_x^2 (kept as constant, $v_x = 200$ km/h, to minimize noise) as input, and cabin lateral acceleration, a_y, as output.

$$a_y^{steer}(t) \;=\; Re(\mathcal{F}^{-1}\{\bar{H}_{\delta_{sw}\to a_y^{steer}}\}) * (\delta_{sw}\cdot v_x^2)(t) \tag{3.19}$$

This approach for identifying the excess motion is validated using a data flow model with a simple one-track model, the schematics are shown in Figure 3.3. A represents a physical vehicle or vehicle model with a yaw moment disturbance, M_z. B can be an identical model, but have $M_z = 0$ as input. B can be used as a reference vehicle model to capture the vehicle motion due to steering. The mathematical expression of M_z can be given by the formula:

$$M_z(t) \;=\; 2\cdot\sin\left(2\pi(t-5)\right)\exp^{-(t-5)} \quad \forall t \in [0,T] \quad \text{else} \quad M_z = 0 \tag{3.20}$$

Where T is the total disturbance time.

The driver model used follows the equation:

$$\delta_{front\,axis}(t) \;=\; -\psi_{vh}(t) - \tan^{-}1\left(\frac{y_{vh}}{v_x\zeta}\right)(t) + \text{noise} \quad \forall\left(\frac{y_{vh}}{v_x\zeta}\right) \in [-\pi,\pi] \tag{3.21}$$
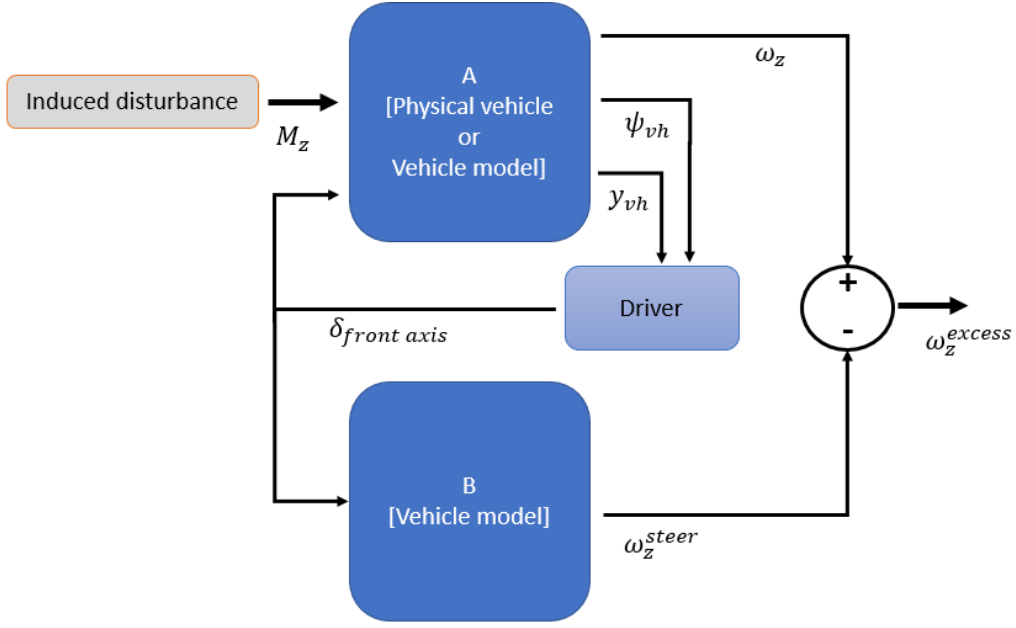
Figure 3.3: *Data flow model on vehicle model with a yaw moment disturbance, M_z.*

Where, $\delta_{front\,axis}$ is the steering angle at front wheels, ψ_{vh} is the yaw angle of the vehicle, y_{vh} is the lateral displacement of the vehicle and $v_x\zeta$ is the look-ahead distance for the driver to correct back to the straight line. The resulting amplitude of $\omega_z{}^{excess}$ is compared between the output from the proposed approach and that from the Simulink model, which will be discussed in Section 4.4.

3.2 Experiment design

The present study utilizes on-road and driving simulator experiments. The initial experiment trial was on-road (Paper A), and was conducted to find post-processing approaches to relate the subjective evaluation of perceived stability to measurable quantities such as steering responses, and linear and rotational motions between configurations. After Paper A, more knowledge was needed to understand what events drivers react to and be able to pinpoint when they occur without all the on-road noise. As a result, a driving simulator trial (Papers B & C) was conducted. The purpose is to build a region of interest for external excitations in terms of frequencies and amplitudes and to develop a model that predicts the drivers' ability to identify the presence of any induced excitation. The final trial (Paper D) was done again on-road to further understand the excitation and driver response on more realistic road conditions and compare the derived predictive model from on-road data with that from the driving simulator data. This chapter covers the experimental setups used for both types of trials.

3.2.1 Test vehicles and vehicle setups

For the initial on-road experiment (Paper A), the test object was a mid-size, front-wheel drive sedan, Volvo S60 (model year 2013). The trial was designed to create substandard perceived stability using sets of aerodynamic devices increasing the aerodynamic rear lift coefficient and changing the lift distribution of the test vehicle. The front-wheel-driven version has a

more forward load distribution, compared to a four-wheel-driven version, hence enhancing the sensitivity in the rear due to lower traction on the rear tires. The drivers were simply asked to respond if they perceived poor stability. The differences in the perceived stability were then presumed to be because of the changes to the car using aerodynamic devices. Three devices were selected for this study. The devices are shown in Figure 3.4 and described below:

- Anti-diffuser [a]: Designed with the intention to guide the flow downwards, resulting in increased rear lift, and partially restrict the flow along the diffuser region, Figure 3.4(a).
- Inverted wing [w]: A rear wing attached to act like aircraft wings, set to increase rear lift, Figure 3.4(b).
- Inverted wing with fin [w-f]: A fin placed 90° to the upstream flow as an addition on the left side of the inverted wing to generate asymmetric forces and moments, Figure 3.4(c).

The above-mentioned devices were paired with an additional aerodynamic device termed as Side-kicks [s], Figure 3.4(d). These were shaped as slightly ramped-up separation edges on both sides of the rear bumper, creating an outwash while separating the flow along a clearly defined line.

Despite these extreme modifications on the test vehicle, no alarming instabilities were sensed by the test drivers, which was the prior intention. Wind tunnel tests were later conducted at the
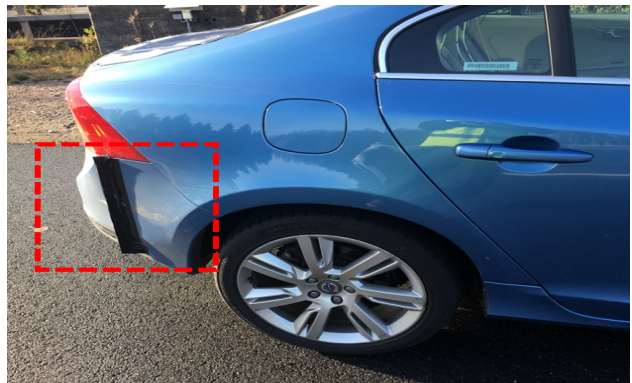

(a)

(b)

(c)

(d)

Figure 3.4: *Aerodynamic devices designed to create substandard perceived stability: (a) Anti- diffuser [a], (b) Inverted wing [w], (c) Inverted wing with fin [w-f], and (d) Side-kicks [s].*

Table 3.1: *The change in mean aerodynamic lift coefficients of each configuration compared to the reference vehicle.*

| | (Δ = Configuration - base car value) | |
| | front lift coefficient | rear lift coefficient |
Configuration	ΔC_{lf}	ΔC_{lr}
Anti-diffuser [a]	-0.001	0.005
Anti-diffuser [a] + Side-kicks [s]	0.000	0.004
Inverted wing [w]	-0.016	0.096
Inverted wing [w] + Side-kicks [s]	-0.016	0.093
Inverted wing with fin [w-f]	-0.012	0.072
Inverted wing with fin [w-f] + Side-kicks [s]	-0.012	0.070

Uncertainty for $\Delta C_{lf} = \pm 0.0015$ *and* $\Delta C_{lr} = \pm 0.008$

Volvo Cars's wind tunnel [57] to obtain the aerodynamic coefficients of each configuration. The change in aerodynamic coefficients of front and rear lifts compared to the reference vehicle are shown in Table 3.1. With the uncertainty of difference between two measurements measured by wind tunnel balance during the same test, shown in Table 3.1, the anti-diffuser [a] showed no change in aerodynamic coefficients of front and rear lifts. For the remaining aerodynamic devices, [w] and [w-f], the changes were significantly higher. The addition of a side-kicks [s] did not make much difference to the front or rear lift coefficients in any of the cases with respect to the uncertainty of the wind tunnel measurements.

The driving simulator trials investigated driver response when driving a compact front-wheel driven SUV. First, a pre-study was done at the Volvo Cars driving simulator. The pre-study adapted the Volvo XC40 vehicle dynamics properties. The real-time vehicle simulation environment was performed using CarRealtime [58]. The final clinical trial was done at the Swedish National Road and Transport Research Institute (VTI). It used a generic vehicle dynamic model that was tuned to behave similarly to the pre-study model in specific maneuvers such as sinusoidal yaw moments with linearly increasing frequencies. The vehicle response output from the pre-study online simulations using CarRealtime of these maneuvers was used for reference. However, the tuned model has its limitations such as generic steering and tire model. The vehicle dynamics model used was originally developed by Bruzelius et al. [59] and refined by Obialero [60]. Coefficients for aerodynamic forces and moments were taken from wind tunnel tests performed earlier and translated to the center of gravity of the vehicle. Noise was added to the experience to create a feeling of road unevenness and was derived from the Inertia Measurement Unit (IMU) readings of the on-road test in Paper A. White noise was filtered to get the desired frequency spectra that matched the accelerations from the on-road data. For simplicity, only the vertical and pitch accelerations were used. Feeding the excitations on each wheel independently is more realistic. However, the available setup and time constraints resulted in feeding them at the center of gravity (CoG) of the vehicle.

The final on-road trial was conducted using a front-wheel-driven XC60 (model year 2015). The trial was done with four different aerodynamic rear spoilers. Spoiler designs A, B, and C shown in Figure 3.5 were selected as suitable candidates for this study based on previous wind tunnel work performed by the aerodynamics group at Volvo Cars. Spoiler D was a late
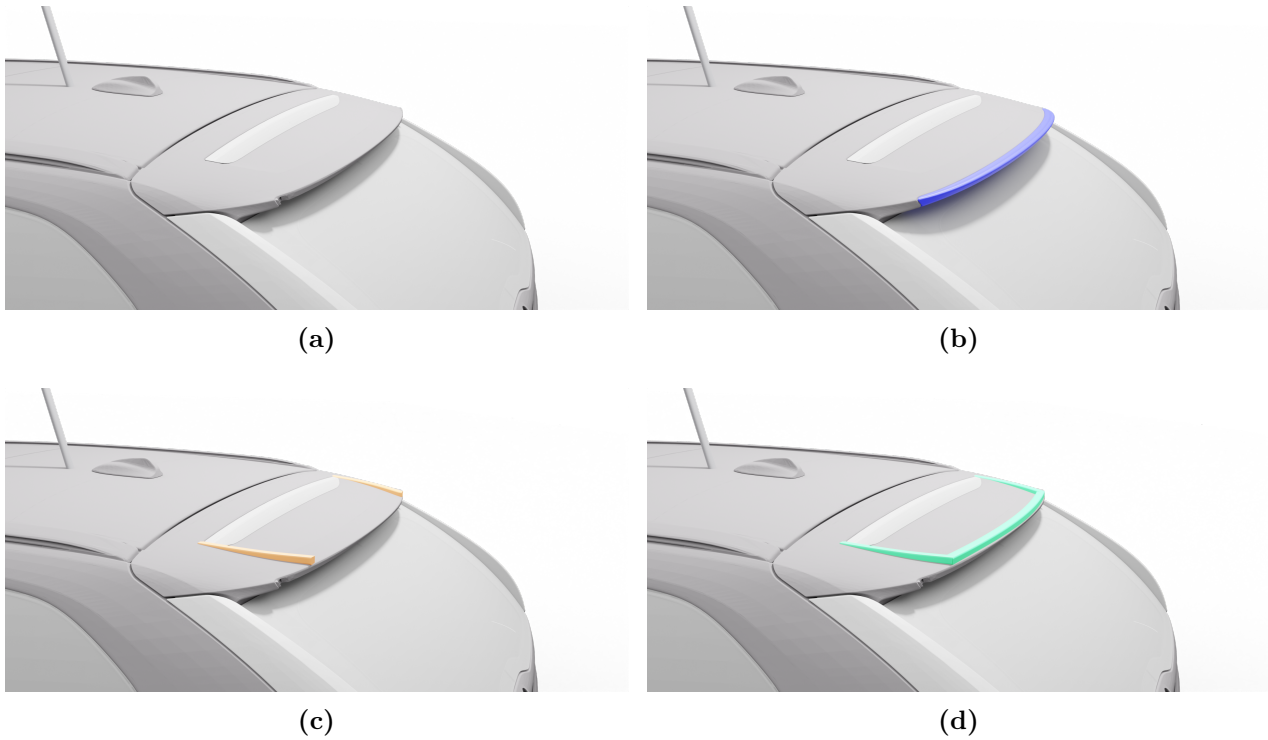
Figure 3.5: *Aerodynamic devices: (**a**) Spoiler A, (**b**) Spoiler B, (**c**) Spoiler C, and (**d**) Spoiler D.*

addition to the test. Apart from the rear lift coefficient C_{lr} of spoiler A, no large differences in mean aerodynamic coefficients between each spoiler were found [61]. However, the subjective evaluation of these spoilers varied during the on-road trials.

3.2.2 Instrumentation

For on-road trials, different variables were recorded through sensors to capture the vehicle's behaviour. A steering wheel torque and angle transducer, from PM Instrumentation [62], measured the steering angle, steering rate, and steering torque and was placed on the steering wheel. The sensor has an uncertainty of ± 0.01 deg. In addition, a trigger button was added on the steering wheel in the final on-road trial (Paper D) to record the drivers' notification of subjectively identifying the presence of external excitations. An Aeroprobe and pressure sensors measured headwind conditions such as yaw angle, roll angle, and angle of attack with a range of ± 70 deg and an accuracy of ± 1 deg. It was positioned 360 mm vertically above the center of the vehicle roof, in line with tests done by Oettle et al. [63]. In the initial on-road trial (Paper A) four laser sensors were installed to measure the ride heights of the test vehicle. Two were placed on the underside of the front and rear bumpers flush with the exterior surface. The remaining two sensors were placed to the sides at the middle of the wheelbase. The measurement of uncertainty for the sensor was ± 0.6 mm. The laser sensors were not included in the final on-road trial (Paper D).

An Inertia Measurement Unit (IMU) was placed in the CoG of the vehicle except vertically (due to structural hindrances). However, the IMU can translate the readings of any reference point on the input, irrespective of the position of IMU itself. A GPS sensor was integrated into

(a)

(b)
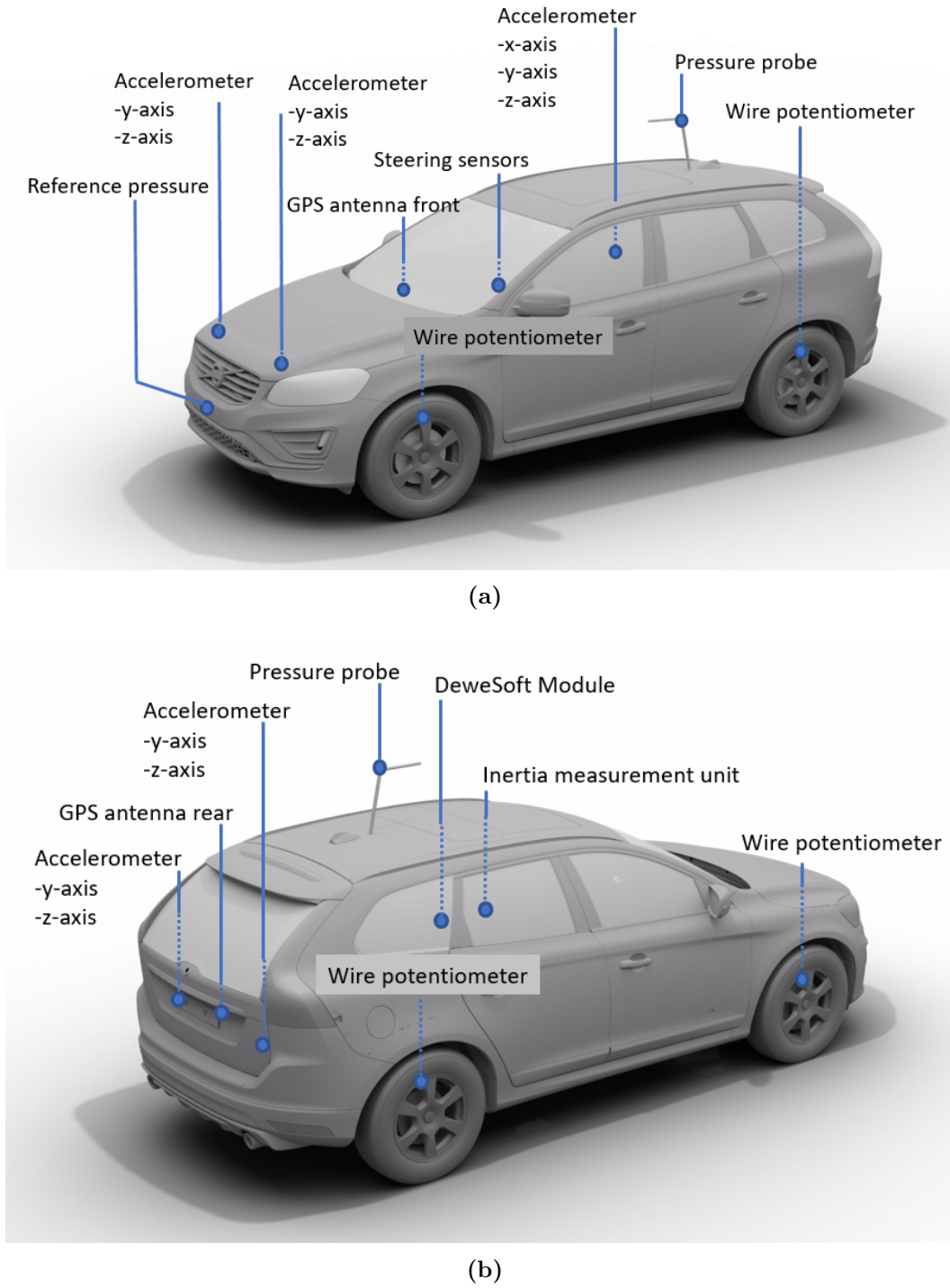
Figure 3.6: *Instrumentation setup for the on-road tests: (a) Front iso view, and (b) Rear iso view.*

this system and the GPS antennas were positioned as recommended by Dewesoft [64]. Four draw-wire potentiometer sensors were co-aligned with the spring of each wheel measuring the displacement of the suspensions with an uncertainty of ±0.03 mm. In Paper A CAN signals from the vehicle's built-in sensors were also recorded. The absolute steering wheel angle data considered in this paper during post-processing were recorded from the CAN bus. The accuracy of these sensors was ±0.1 deg. In Paper D, additional accelerometers were mounted on each
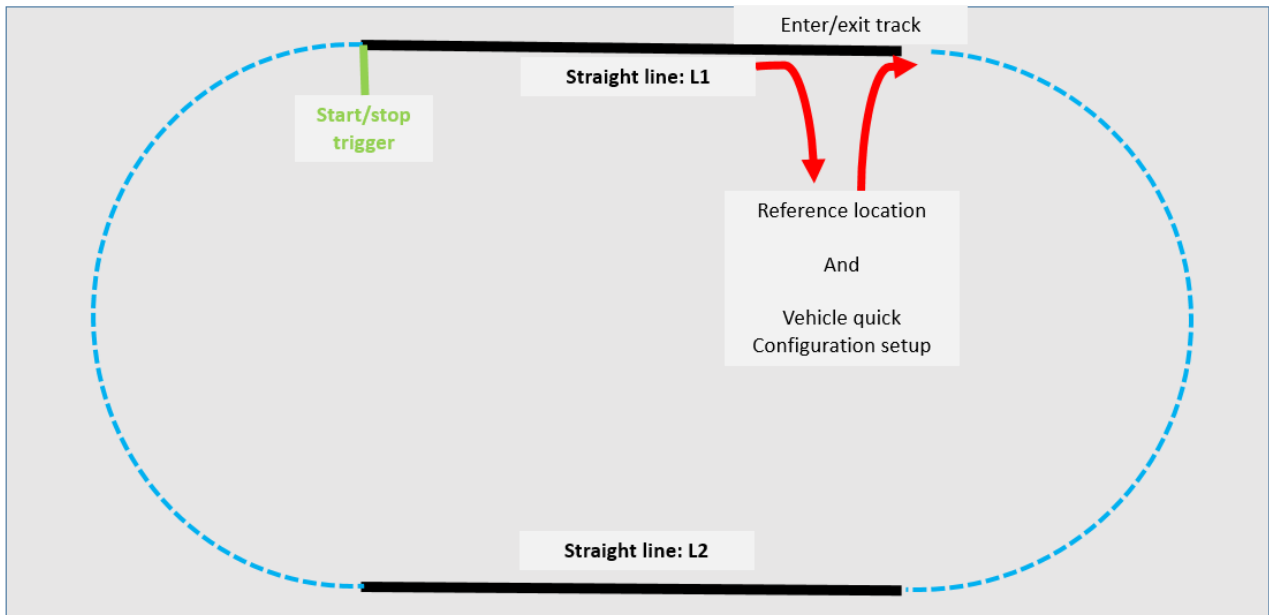
Figure 3.7: *Schematics of the test track at Volvo Cars Hällered Proving Ground.*

corner of the vehicle, detecting the lateral and vertical accelerations of the vehicle. A 3-axis sensor was fixed to the headrest to measure the motion felt close to the driver's upper body. All sensors were connected to a Sirius Dewesoft data acquisition system which timestamps the sensors' readings in a synchronized way. The DewesoftX software was used for data acquisition and some post-processing. The overview of sensors used in Paper D is shown in Figure 3.6.

For driving simulator trials (Paper B & C) the IMU and accelerometers were the only sensors used to measure cabin motion. The other signals such as vehicle motion, steering angle, and drivers' subjective evaluations of excitations were obtained from the simulator. The sensor (i.e. buttons) to measure driver subjective evaluations was also mounted on the steering wheel.

### 3.2.3   Experimental trial design

The study considered a straight-line high-speed driving condition at constant speeds. Each trial run with a driver was shorter than 15 minutes to minimize the potential impact of driver fatigue [51, 52]. The drivers were asked to keep the vehicle in a straight line. The on-road studies were carried out at Volvo Cars Hällered Proving Ground. It is an oval track with two straight lines (L1 and L2) of 1.1 km, as sketched in Figure 3.7. In the study, the data analysis only considered measurements along the two straight lines. The signals were tared at a reference position on the track i.e., the values at this point were set as offsets. The car was modified with aerodynamic devices to the desired configuration at this reference position.

The initial on-road experiment (Paper A) was performed with three test drivers. This test focused on the subjective evaluation of the vehicle's perceived stability under minimal wind conditions. The test was conducted on days with minimal wind conditions (< 3 m/s) and the start of data acquisition was triggered when the desired speed is achieved. For each configuration, the trial run was over after three full laps of the high-speed track. Only data

sampled at speeds of 230 and 250 km/h was analyzed. The variables considered for the study were lateral acceleration a_y, yaw velocity ω_z, steering angle δ_{sw}, and steering torque τ_{sw}. The influence of heave and roll velocitys under these driving conditions was negligible, hence, they are not further discussed.

In the final experimental trial in the driving simulator study (Paper B & C) 23 drivers were asked to keep a straight line at a constant speed of 200 km/h and evaluate their experience while the car was experiencing induced disturbances. The drivers were categorized into common and professional test drivers. The common drivers were 13 in total with 82% men and an average age of 33 (± 8) years. Their average driving experience was 14 (± 6) years. The professional test drivers were 10 in total. All were men with an average age of 40 (± 11) years and average professional driving experience of 16 (± 9) years. The limited number of participants is not representative for the general population. However, the goal of the study is to be able to predict subjective evaluation made by professional test drivers before a physical car is built. It is therefore not necessary for the study to be representative of the general population. For subjective evaluation, the drivers were provided with 3 response buttons on the steering wheel, with which the driver could respond: 0 for *'did not feel'*, 1 for *'felt'* and 2 for *'felt and potential instability'*.

The pre-study at the Volvo Cars Driving Simulator helped in narrowing down the amplitude and frequency ranges of interest of the excitations. The excitations induced in this study were in the form of yaw and roll moments acting at the center of gravity of the vehicle. For achieving the selected frequency ranges, a base excitation signal was passed through an 8th-order Butterworth band pass filter. The base excitation is generated using the following equation:

$$y(t) = \text{sgn}\left(\frac{T}{2} - 1\right) \cdot \left(1 - \cos\left(\frac{2\pi}{T} \cdot t\right)\right) \quad \forall \quad t \in [0, 10] \qquad (3.22)$$

where, y is the amplitude at a given time t and $T = 10$ is the total excitation signal time.

The selected frequency ranges were $0.25 - 0.5$ Hz (F1), $0.5 - 1.0$ Hz (F2), $1.0 - 2.0$ Hz (F3), and $2.0 - 4.0$ Hz (F4). And the signal of selected frequency ranges was multiplied with the desired amplitudes: 150 Nm (A1), 175 Nm (A2), 225 Nm (A3), and 325 Nm (A4). This results in 16 unique excitation signal combinations of interest in this study. These signals were fed to the simulator in the form of pure roll or yaw moments. As a result, a driver experienced with 32 distinct signals: 16 unique yaw and roll moments. They were randomly ordered into 23 unique sequences. The overview of the drivers' evaluation of all signals considered in this study is shown in Table 3.2.

Figure 3.8 shows the designing and sequencing layout of the excitations of interest. The road noises and static aerodynamic load were fed throughout the simulation time. The simulation time was split into signal windows around each of the sequenced excitation of interest. Each signal window can be split into two segments: *'Before disturbance'* and *'During disturbance'*. As a result, the rotational rate, ω_i, measured from the cabin at *'Before disturbance'* segments can be considered as ω_i^{steer}, as previously mentioned in Section 3.1.4. All the *'Before disturbance'*

Table 3.2: *Overall distribution of drivers' subjective evaluation to the induced disturbances.*

| | Yaw Disturbances | | Roll Disturbances | | |
| | Driver type | | Driver type | | |
Driver evaluation	Common driver	Test driver	Common driver	Test driver	Total
0 - Did not feel	88	33	150	101	372
1 - Felt	108	68	53	55	284
2 - Felt and potential instability	12	59	5	4	80
Total	208	160	208	160	736
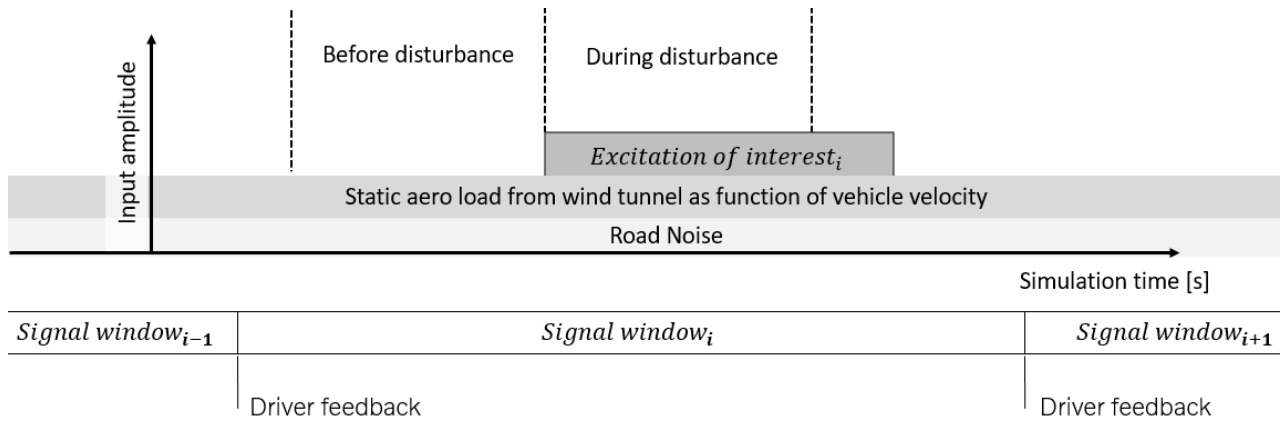
Figure 3.8: *Designing and sequencing layout of excitations of interest.*

segments from the samples are used for deriving the weighted transfer function, $\bar{H}_{\delta_{sw} \to \omega_i{}^{steer}}$ with input signal ω_i filling in for ω_i^{steer}.

In the final on-road trial (Paper D), the participants were 18 professional test drivers that engage in subjective evaluations of vehicle performance during product development. All drivers were male with an average age of 40 (± 11) years and professional driving experience of 17 (± 10) years. The trial runs with the four spoiler configurations were sequenced in the same order for each driver and performed at a constant cruising speed of 200 km/h. The drivers were asked to press the button on the steering wheel when an excitation was felt. Unlike in the driving simulator trial design, there is no clear undisturbed time sequences similar to the *'Before disturbance'* segments for deriving the weighted transfer function, $\bar{H}_{\delta_{sw} \to \omega_i{}^{steer}}$.

For developing the predictive models, an algorithm was used for variable selection through iteration run over combinations of independent variables to find the highest significance (p-value).

3.2.4 Further insights of trial design

This section explains some of the challenges and differences in the design layout of trial designs in both driving simulator and on-road trials.

Driving simulator trial design

It is challenging to achieve large sample sizes of trials and enough drivers who participated to represent the general population. With the sample of common drivers and professional test drivers used in this work, a projection of the difference in their steering behaviour and sensitivity to excitations is observed. Professional test drivers are expected to be more sensitive to vehicle instabilities and more consistent in their evaluation than common drivers.

In the driving simulator study (Paper B & C) the induced excitations act on the CoG of the vehicle. They stimulate the drivers closer to a sensation of pure roll moment or yaw moment. These excitations are not simulating the whole force and moment situation in all frequencies in a real on-road scenario but the motivation behind this component-wise approach is to identify the dominating variables along with the frequency ranges and amplitudes that will trigger the drivers' perception of instability. Once identified, it will be easier to filter data from future studies for further investigation.

The experiment trial in the simulator study lacked control trials to measure the level of bias of participants' response to zero excitation. For indicating the level of bias, the subjective evaluation of the least sensitive excitations is used to indicate a maximum level of bias, i.e., the level of 1 or 2 responses when there is no induced disturbance. Roll moment excitations at frequencies F1 $(0.25 - 0.5$ Hz$)$ and F2 $(0.5 - 1$ Hz$)$ and the lowest amplitude A1 $(150$ Nm$)$ were used for this purpose. Considering all drivers, the bias may be up to 16% $(\pm 7\%)$. The overview of the drivers' evaluation suggests that the second level of the response scale, 2 - *'felt and potential instability'*, may lack reliability, but merely feeling the disturbance should be easy to understand. Therefore, the two levels were merged into one for analysis: 0 for *'did not feel'* and 1 for *'felt'* and *'felt and potential instability'*.

The road noise fed to the driving simulator was in the form of vertical acceleration and pitch moment at the CoG of the vehicle. There were no externally added forces and moments acting on the car between induced excitations. The results show that the drivers' reaction to the excitations is not significant. The ω_x^{excess} and ω_z^{excess} represent rotations in excess of that directly resulting from steering input calculated using a transfer function and depend on the interaction between vehicle, driver and external excitations.

On-road trial design

The final trial on-road (Paper D) only had the professional test drivers as participants. As a result, the model derived relates to the subjective evaluation of professional test drivers.

Unlike the set-up in the driving simulator, road noise acts on all four wheels in the on-road test. As a result, all components of road noise were significantly higher than that of the driving simulator test, further discussed in Section 4.3.2. The $\omega_{x,std}$ and $a_{x,std}$ values showed the highest relative increase. Moreover, unlike in the driving simulator, the excitations were a result of

the natural environment and road and were not triggered and shaped in a controlled manner. The transfer function used to estimate ω_i^{excess} was therefore calculated as a weighted mean of transfer functions from all drives along straight lines, but separately for each trial, to minimize bias from transient external excitations.

4

Results and discussions

This chapter summarizes the findings from all the tests conducted in this study. The first on-road test (Paper A) gave an overall understanding of the relation between the driver and measurable quantities. Visual tools that differentiated subjective evaluation of drivability within paired aerodynamic configurations with measured variables were presented. The details will be further discussed below. The driving simulator and final on-road tests (Paper B, C & D) developed predictive models. These tests investigated the characteristics of measured variables in terms of amplitude and frequencies and their influence on the drivers' ability to identify any aerodynamic excitations.

4.1 Visual representation of subjective evaluation

In the first on-road test (Paper A), major modifications were implemented through aerodynamic devices as explained in section 3.2.1 with the prior intention of inducing significant vehicle instabilities. However, no alarming instabilities were sensed by the test drivers. The vehicle behaviours felt by drivers with the attachment of the three aerodynamic devices:

- The anti-diffuser yielded a more high-frequency yaw disturbance behavior compared to the other configurations.
- The inverted wing gave a low-frequency sway behaviour with the impression that the source of excitation was from the rear end of the test object.
- The inverted wing with fin resulted in a similar behaviour similar to that with just the inverted wing, but in addition, there was a slight leftward yaw.

The test drivers observed an improvement in drivability and the above-mentioned behaviours of the respective configurations were notably dampened with attachment of side-kicks, shown in Figure 4.1. As presented in Table 3.1, the addition of a side-kicks did not make a significant difference to the front or rear lift coefficients for any of the three tested configurations.

The study brought two tools useful for visualizing measurement data that can be connected to subjective evaluations. The first one is the mean and standard deviation vector plots. The vector lines represented in Figure 4.2 show each configuration pair, connecting from the configuration without to with side-kicks. The method is described in detail in Section 3.1.1.

With a straight-line driving scenario, the mean values of lateral acceleration, a_y, and yaw

Notations	Configuration	Drivability good	Drivability poor
a	Anti- diffuser		x
a-s	Anti- diffuser + side-kicks	o	
w	Wing		x
w-s	Wing + side-kicks	o	
w-f	Wing + fin		x
w-f-s	Wing+ fin + side-kicks	o	

Figure 4.1: *Subjective evaluation between paired configurations, where 'good' or 'poor' drivability is relative to the configuration in the same pair.*
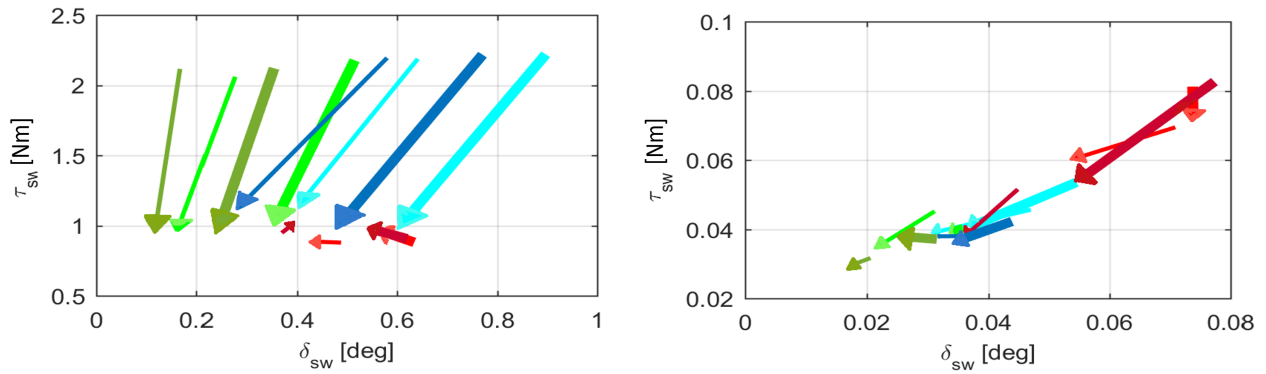
(a) *Mean values*   **(b)** *Standard deviations*

Configurations [Without to with side-kicks(s)]	Straight line	Speed [Km/h]
a to a-s	L1	230
w to w-s	L1	230
w-f to w-f-s	L1	230
a to a-s	L1	250
w to w-s	L1	250
w-f to w-f-s	L1	250
a to a-s	L2	230
w to w-s	L2	230
w-f to w-f-s	L2	230
a to a-s	L2	250
w to w-s	L2	250
w-f to w-f-s	L2	250

Figure 4.2: *Vector plots of mean values (a) and standard deviations (b) of steering torque τ_{sw} vs steering angle δ_{sw} of each straight line L1 and L2 for the different configurations and speeds.*

velocity, ω_z, will be negligible. In the case of steering angle, δ_{sw}, and steering torque, τ_{sw}, the mean value depicted the excess averaged steering input required by the driver in response to exterior disturbances while keeping the test object following the straight line. The vector plots presented in Figure 4.2(a) point towards the origin, implying the lower need for δ_{sw} and τ_{sw} response. This may be an indication of good drivability. These vector plots fall in line with the overall subjective evaluations of all configurations with and without side-kicks except for the anti-diffuser. The standard deviation vector line patterns of τ_{sw} vs δ_{sw} coincides with subjective evaluation for all configurations with and without side-kicks, as shown in Figure 4.2(b). A similar pattern is also found for lateral acceleration, a_y, and yaw velocity, ω_z, shown in Paper A. This suggests that side-kicks dampen the unsteady vehicle behaviour, resulting in better driving in a straight line.

The second tool is the ride diagram method. The plots in Figure 4.3 show the mean squared values (MS) values of the transient part of the signals to the left and the MS values of the remaining stationary part of signals to the right, explained in detail in Section 3.1.2. Unfilled markers represent respective configurations without side-kicks and filled markers represent configurations with side-kicks. The sum of the transient and stationary part gives the total MS value of the signal. The further the MS value is from the origin of the x axis, the lower the standard of drivability. Such an interpretation agrees with the subjective evaluation of all configurations, Figure 4.3.

On the transient side in Figure 4.3(a), the transient nature of the signal is larger in the configuration with anti-diffuser compared to other configurations at 250 km/h. At 230 km/h the transient side of the configuration pair with the anti-diffuser is not predominant and the
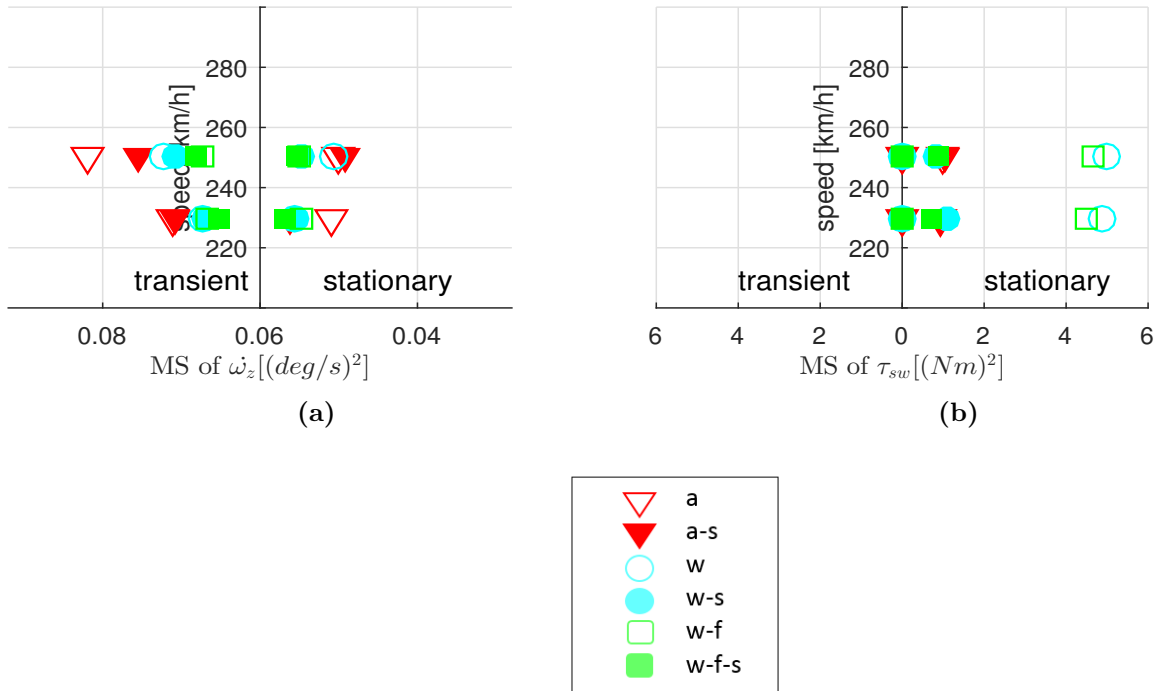

Figure 4.3: *Ride diagram of all configurations and selected speeds:* **(a)** *Yaw velocity ω_z, and* **(b)** *Steering torque τ_{sw}.*

trend is opposite to the subjective judgment by a small margin. However, on the stationary side, the configuration with anti-diffuser, a, is mainly showing a worse trend than the configuration with anti-diffuser and side-kick, a-s. The steering characteristics such as τ_{sw}, Figure 4.3(b), show a larger contribution on the stationary side for wing and wing with fin configurations. The transient contribution in all configurations is negligible in comparison. This shows the inability of the drivers to respond to unknown transient behaviours.

4.2   Drivers' evaluation in driving simulator trial

The driving simulator tests (Paper B & C) showed that the test drivers are more sensitive to yaw excitations at all tested frequency ranges compared to common drivers, Figure 4.4. The

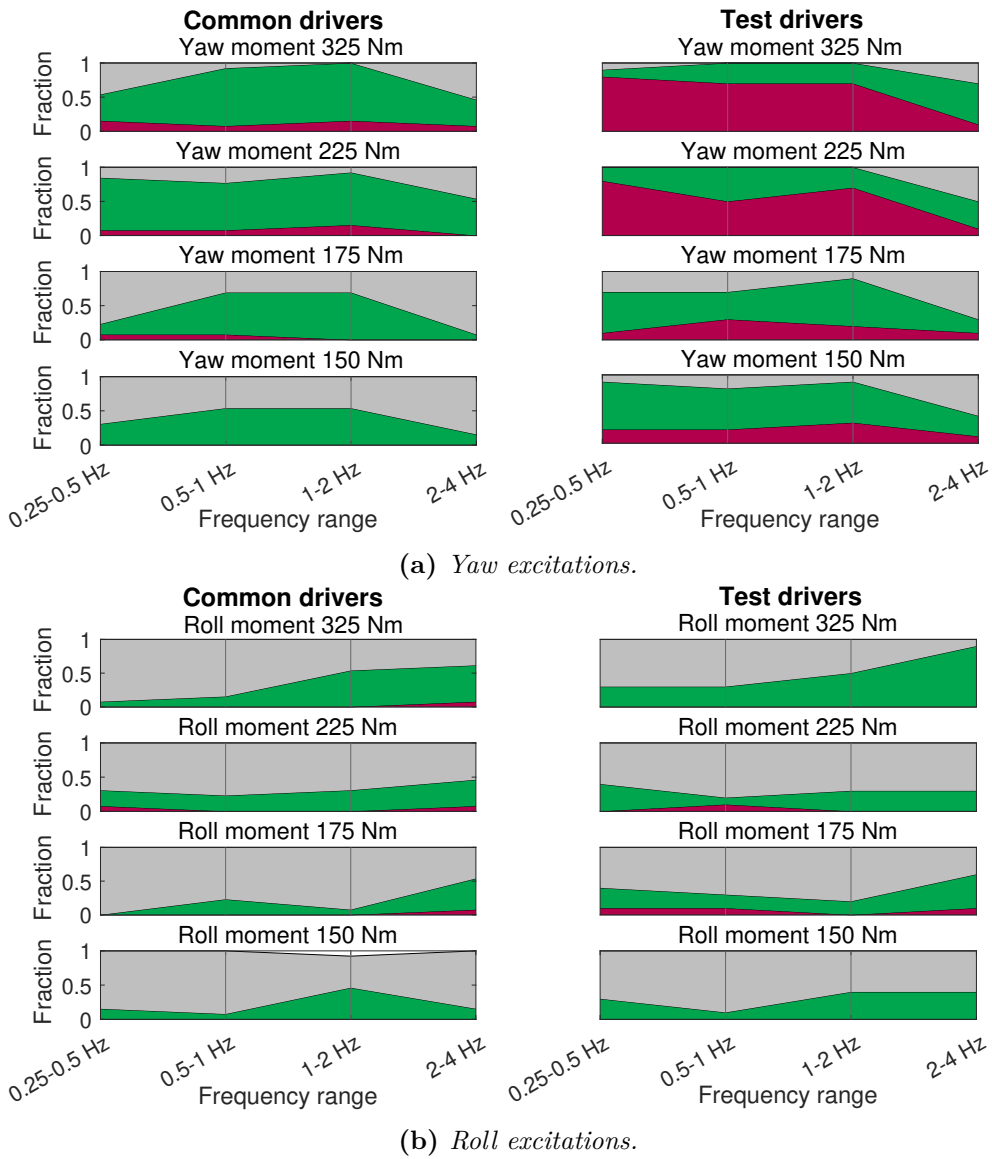**(a)** *Yaw excitations.*

(b) *Roll excitations.*

Figure 4.4: *Stacked fraction of driver responses after yaw and roll moment excitations at different amplitudes and frequency ranges. Legend: grey - 'did not feel', green - 'felt', and red - 'felt and potential instability'.*

responses from test drivers can be seen to transition from 1 (*'felt'*, coloured green) to 2 (*'felt and potential instability'*, coloured red) with increasing amplitude of yaw disturbances. This suggests that test drivers' sensitivity threshold for sensing yaw excitations is lower than the tested amplitudes. But there was no difference in sensitivity between both types of drivers for roll excitations and only transition from 0 (*'did not feel'*) to 1 (*'felt'*) is seen for both types of drivers, which increases with higher amplitude and higher frequency range.

At all tested amplitudes, it is observed that at $2-4$ Hz the drivers' ability to identify yaw excitations drop but the ability to observe roll excitations increase. A reason for this observation is the chassis characteristics as shown by the swam plot of yaw velocity, ω_z, and roll velocity, ω_x, measured in the cabin during yaw and roll excitations respectively. In Figure 4.5 it is observed that the chassis' dampens yaw excitations at $2-4$ Hz. However, $2-4$ Hz lies in the natural frequency range of the roll of the chassis in the case of roll excitations as shown in Figure 4.6. Statistical tests were done separately on tested amplitudes and frequency ranges. The Chi-squared test (χ^2 test, $N = 368$, $df = 3$, p-value < 0.001) of yaw excitations showed
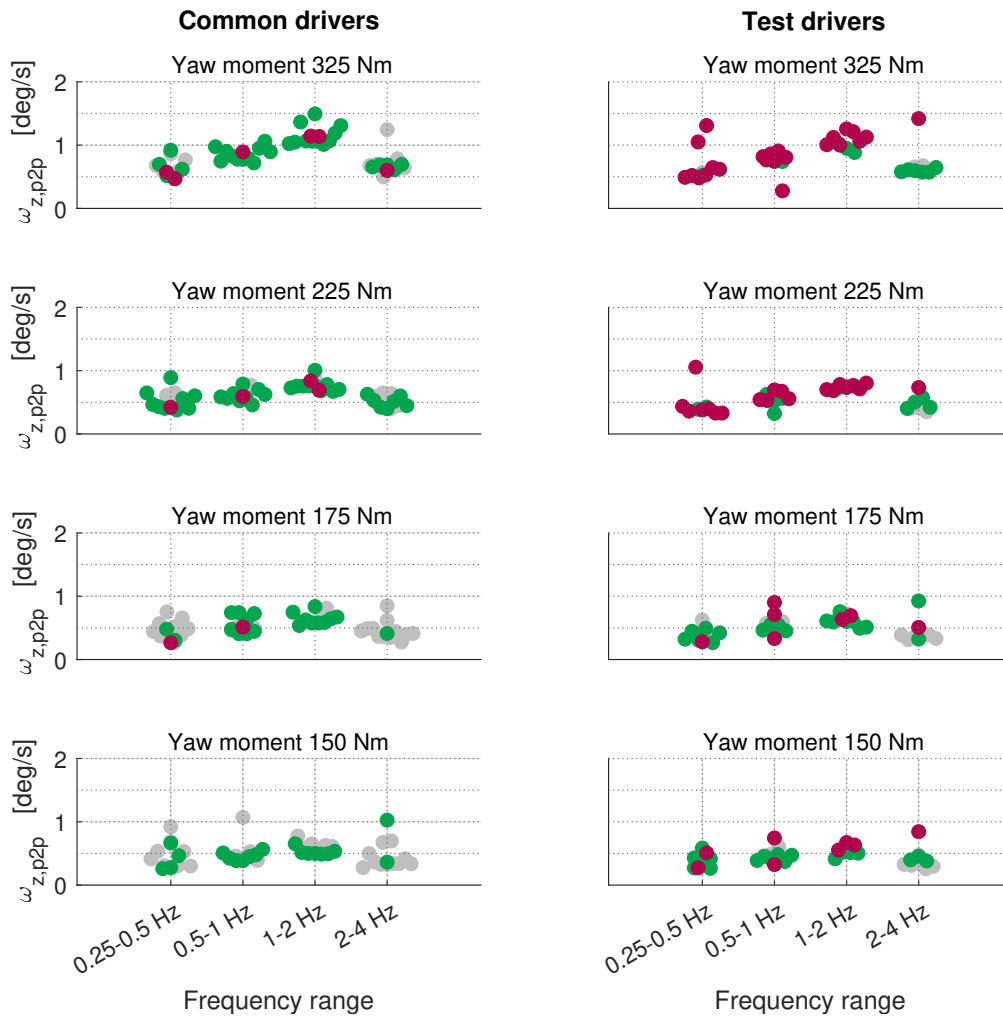

Figure 4.5: *Swarm plot of frequency range vs peak-to-peak yaw velocity, $\omega_{z,p2p}$, vs driver response for different driver type and yaw moment excitation amplitudes. Legend: grey - 'did not feel', green - 'felt', and red - 'felt and potential instability'.*
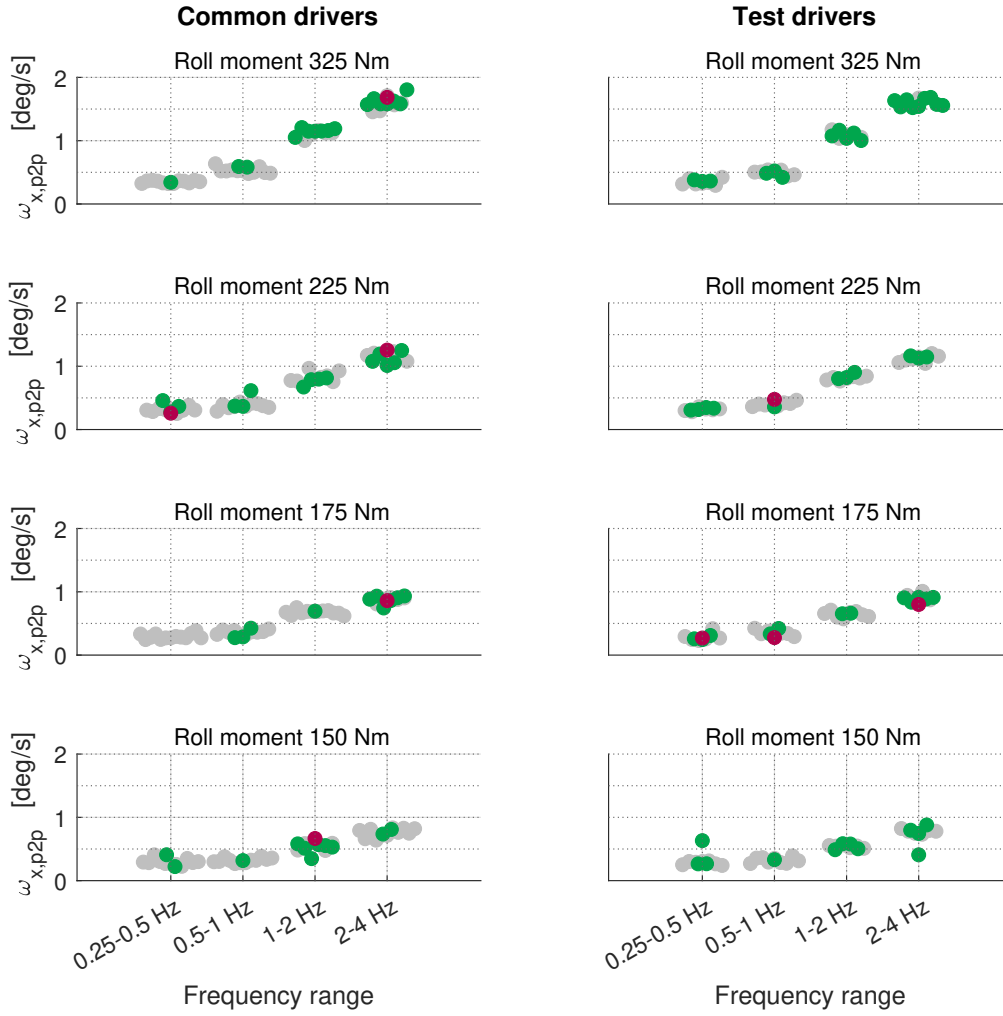
Figure 4.6: *Swarm plot of frequency range vs peak-to-peak yaw velocity, $\omega_{x,p2p}$, vs driver response for different driver type and roll moment excitation amplitudes. Legend: grey - 'did not feel', green - 'felt', and red - 'felt and potential instability'.*

significant relation of the driver response to both the tested frequency ranges and amplitudes. However, the χ^2 test of roll excitations showed significant relation of the driver response to the tested frequency ranges ($N = 368$, $df = 3$, p-value < 0.001) but not to the tested amplitudes ($N = 368$, $df = 3$, p-value $= 0.12$). Even so, both figures show that a selected excitation with a given amplitude results in a distribution in amplitude for the resulting vehicle body rotation $\omega_{i,p2p}$. Hence, because of road noise, driver input, vehicle dynamics and motion queuing, the conditions under which every sample is taken is unique. There is an overlap in measured amplitudes of yaw velocity between different amplitudes of excitation. This partially explains why there are different subjective evaluations to the same induced excitation. No explanation relating the difference in driver subjective evaluation can be deduced when considering only peak-to-peak or standard deviation of rotational rate, ω_i. Since there is a distribution of measured amplitudes from the IMU, rather than distinct points, a regression is a suitable approach and will be applied in the next section.

Figure 4.7 represents the steering characteristics before and during the excitations. The steering
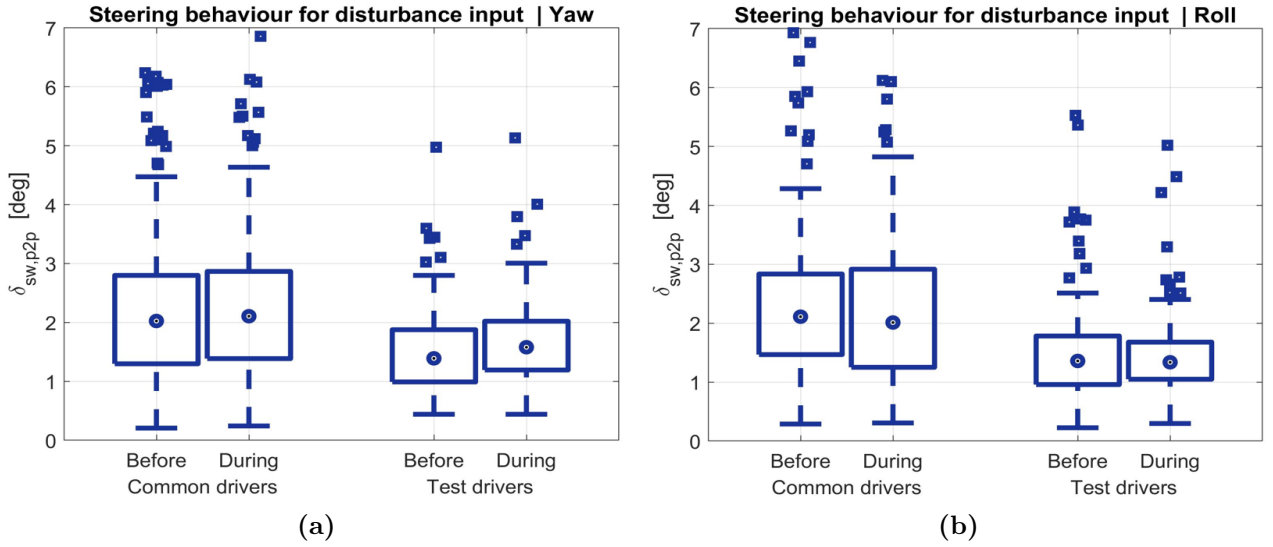
Figure 4.7: *Box plot of peak-to-peak steering angle, $\delta_{sw,p2p}$, characteristics depending on driver type Before and During disturbance segments for: (**a**) Yaw moment excitations and (**b**) Roll moment excitations.*

was not significantly larger during the excitations compared to before the excitations, i.e., the greater steering especially observed in common drivers is not a result of the excitations. The higher inputs from steering might create an anticipated vehicle behaviour making them less sensitive to induced excitations. This could partially explain why common drivers are less sensitive to induced excitations than test drivers.

4.3   Predictive model

The predictive model was created from logistic regression by building the relation between drivers' subjective evaluation as the dependent variable and measured vehicle motion variables as independent variables (predictors).

The influence, I, is a term introduced to understand further about each predictor of a given predictive model. I for a given predictor, k, is defined as the ratio between the impact of model parameter, β_k, of a change of a given predictor on the log-odds, times its standard deviation, $x_{k,std}$, and the sum the numerator for all predictors. The influence, I, for a given predictor, k, is given by the equation:

$$I_k \;=\; \frac{|\beta_k \cdot x_{k,std}|}{\sum_{i=1}^{n}|\beta_i \cdot x_{i,std}|} \tag{4.1}$$

4.3.1   Predictive model from driving simulator test

For the predictive model from driving simulator, standard deviation values of 5 second windows of before and during disturbances of the measured variables of each excitation were used as

independent variables and respective drivers' subjective evaluation is assigned as dependent variable. The predictive model was optimized by considering only independent variables with high level of significance i.e., p-values < 0.001. The resulting optimized independent variables were roll velocity $\omega_{x,std}$, yaw velocity $\omega_{z,std}$, steering angle $\delta_{sw,std}$ and driver type c_{DT}. The resulting predictive model, $p(z)$, has an overall accuracy of 85.5% to predict the drivers' ability to identify an excitation, and its' properties are shown in Table 4.1.

The negative β coefficient for steering angle indicates that the drivers' sensitivity reduces with steering fluctuations, supporting the observation previously mention about Figure 4.7. Replacing $\omega_{z,std}$ with standard deviation of excess yaw velocity $\omega_{z,std}^{excess}$, the predictive model improved its overall accuracy from 85.5% to 87.5%. A similar replacement for roll velocity didn't show significant improvement. The updated predictive model property is shown in Table 4.2. The p-values became smaller with excess compared to Table 4.1, which states the increase in the level of significance of the variables in the model.

I is reduced by half for $\delta_{sw,std}$ hence reducing the direct impact of driver-vehicle interaction on the predictive model. On the other hand, I of yaw and roll variables have increased significantly. This implies that a driver is mostly sensitive to rotational rate impulses that cannot be predicted from steering and therefore are unexpected. Independent variables based on excess rotational rate, i.e., rotational rate not caused by steering, are the strongest investigated predictors for a driver to identify an excitation. When using the direct rotational rate, any driver input adds noise to the rotational rate signals decreasing the ability to predict what excitations a driver can feel.

Table 4.1: *Properties of the predictive model from driving simulator with direct variables*

	β_k	p-value	I_k
offset	-5.86 [-]	$0.24 \cdot 10^{-46}$	-
$\omega_{x,std}$	21.60 [s/deg]	$0.27 \cdot 10^{-26}$	0.13
$\omega_{z,std}$	61.94 [s/deg]	$0.66 \cdot 10^{-57}$	0.45
$\delta_{sw,std}$	-7.81 [1/deg]	$0.24 \cdot 10^{-40}$	0.34
c_{DT}	0.86 [-]	$0.77 \cdot 10^{-08}$	0.07

Table 4.2: *Properties of the predictive model from driving simulator after replacing direct variables with excess motion variables*

	β_k	p-value	I_k
offset	-6.68 [-]	$0.92 \cdot 10^{-50}$	-
$\omega_{x,std}^{excess}$	25.05 [s/deg]	$0.20 \cdot 10^{-31}$	0.20
$\omega_{z,std}^{excess}$	70.05 [s/deg]	$0.11 \cdot 10^{-65}$	0.53
$\delta_{sw,std}$	-2.79 [1/deg]	$0.22 \cdot 10^{-15}$	0.17
c_{DT}	0.79 [-]	$0.22 \cdot 10^{-06}$	0.09

Table 4.3: *Properties of the predictive model from driving simulator with excess motion variables and significant ranges of studied frequencies*

	Frequency range [Hz]	β_k	p-value	I_k
offset		-6.69 [-]	$0.26 \cdot 10^{-44}$	-
$\omega_{x,std}^{excess}$	0.25-0.5	73.51 [s/deg]	$0.21 \cdot 10^{-09}$	0.08
	1-2	25.31 [s/deg]	$0.13 \cdot 10^{-11}$	0.09
	2-4	22.45 [s/deg]	$0.37 \cdot 10^{-12}$	0.09
$\omega_{z,std}^{excess}$	0.25-0.5	63.14 [s/deg]	$0.77 \cdot 10^{-21}$	0.14
	0.5-1	52.20 [s/deg]	$0.29 \cdot 10^{-15}$	0.16
	1-2	53.55 [s/deg]	$0.48 \cdot 10^{-13}$	0.19
	2-4	55.01 [s/deg]	$0.14 \cdot 10^{-09}$	0.08
$\delta_{sw,std}$	1-2	-7.86 [1/deg]	$0.89 \cdot 10^{-09}$	0.09
c_{DT}	-	0.84 [-]	$0.11 \cdot 10^{-06}$	0.07
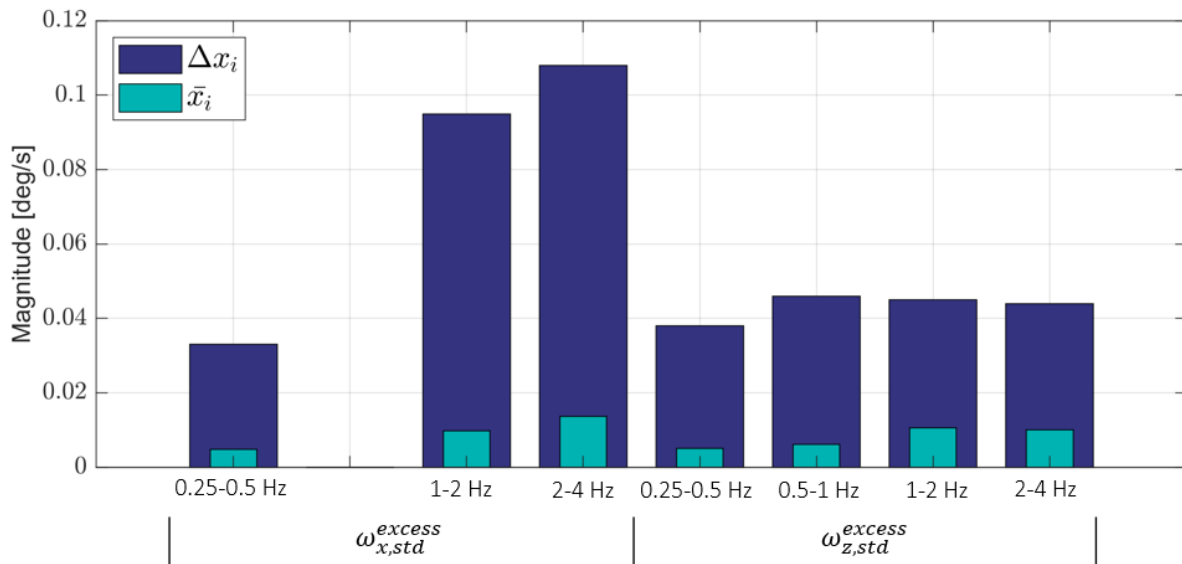
Figure 4.8: *Additional magnitude required for each rotational rate variable, Δx_i, in Table 4.3 to increase probability of feeling the excitation, $p(z)$, from 3% up to 75%. Lower magnitude of Δx_i implies higher sensitivity of respective variable, x_i, in the predictive model*

Further investigation of the independent variables of the model was made with the focus on the impact they have over the tested frequency ranges. Table 4.3 shows the model properties. It has an overall accuracy of 87.5%. The model suggests that drivers are most sensitive to yaw velocity. This is inline with previous studies [37, 38, 65]. The improved predictive model also shows that the yaw velocity plays a significant role throughout the studied frequency range $0.25 - 4$ Hz. The influence of steering input from the drivers is significant only around to $1 - 2$ Hz. Since the excitations designed for the driving simulator were intended as a pure moment component acting on the CoG of the vehicle, $a_{y,std}^{excess}$ and $\omega_{z,std}^{excess}$ are highly correlated. As a result, the accuracy of the model shown in Table 4.3 remains nearly unchanged when $a_{y,std}^{excess}$

replaces $\omega_{z,std}^{excess}$ as an independent variable. The frequencies of significance of the variables also remain the same.

Figure 4.8 shows the additional magnitude required for each rotational rate variable, Δx_i, in Table 4.3 when considered individually, to increase the probability of feeling the excitation, $p(z)$, from 3% up to 75%. z represents the log-odds. The mean magnitude of standard deviation of samples of rotational rate variables is denoted as $\bar{x}_i$. A lower magnitude of Δx_i represents higher sensitivity of respective variable, x_i, in the predictive model. In addition, a new finding shows that the drivers' sensitivity to roll velocity in the frequency range of 0.25-0.5 Hz is comparable to the yaw velocity. The improved model provides a clearer understanding of the threshold of excitations of various frequencies and disturbance type that will influence the drivers' perception towards vehicles stability and nervousness.

4.3.2   Predictive model from on-road test

The box plot of standard deviation of each variable measured in the driving simulator and on-road tests over the 5 second window samples is shown in Figure 4.9. The difference in magnitude distribution of variables $\omega_{y,std}$ and $a_{z,std}$ between driving simulator and on-road are relatively low. This is a result of how the road unevenness were implemented in the driving simulator test setup, as discussed in Section 3.2. The magnitude was fine-tuned subjectively due to the hexapod physical limitations. Considering the condition that the road unevenness spectra were not fed at wheel centers and only vertical, and pitch components were simulated, the significant difference in magnitude distribution of $\omega_{x,std}$ is self-explanatory. From the comparison of $\omega_{z,std}$ and $a_{y,std}$, the disturbances simulated in the simulator appear close to what was experienced on-road. Although from the figure, the steering angle, $\delta_{sw,std}$, aligns with respect to the magnitude distribution, it isn't relatable. From the results, it is observed that for small δ_{sw} inputs the steering to vehicles motion gain (input to output gain) of the driving simulator steering model is significantly higher than the on-road steering system. This
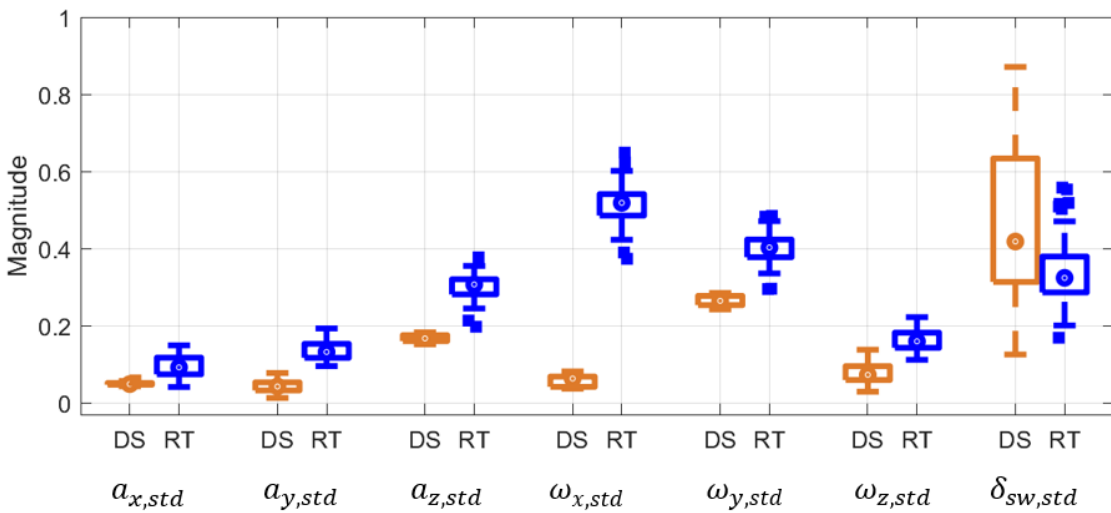

Figure 4.9: *Box plot comparison between the driving simulator study (DS) and on-road study (RT) on standard deviation magnitudes of road noises and steering noises over 5 second window samples.*

implies that small δ_{sw} input in the on-road test resulted in lower vehicle motion compared to the driving simulator test.

For the predictive model from the on-road data, 5 second windows ending at the time at which the driver had pressed the button were extracted for each button press and categorized as having felt the presence of external excitation. The remaining data was split up into 5 second non-overlapping windows with a 2.5 second margin to already extracted data and categorized as undisturbed. The independent variables in the predictive model, obtained from the iterative process as mentioned in Section 3.2.3, contain the standard deviation value of the 5 second windows representing the respective dependent variable. The resulting predictive model properties with independent variables similar to that of the driving simulator study are shown in Table 4.4.

The model with excess variables obtained from on-road data, Table 4.4 can be compared to that from the driving simulator, Table 4.3. The model coefficients, β, are lower in the on-road model than in the driving simulator model implying the need for larger excitations to trigger a driver's sensitivity. This is quite expected since there is more noise on the road compared to the driving simulator scenario, as previously discussed. Unlike the excitations induced in the driving simulator, the excitations experienced on-road consist of pressure and shear forces acting non-uniformly across the vehicle together with excitations from road unevenness. Nevertheless, in the on-road model, the lateral motions $\omega_{z,std}^{excess}$ and $a_{y,std}^{excess}$ are highly correlated. The comparison between models confirms that the yaw moment is important in the $0.5 - 2.0$ Hz range, consistent with the results from the driving simulator. This observation on the importance of yaw moment agrees with the findings from the studies by Huemer et al. [37], Nguyen et al [38], and Brandt et al. [65].

The impact of excess roll velocity, $\omega_{x,std}^{excess}$, presented by the model from the driving simulator contradicts that by the on-road study. The model coefficient, β, of $\omega_{x,std}^{excess}$ in Table 4.4 is negative which implies the presence of $\omega_{x,std}^{excess}$ decreases the probability to identify the excitation in the on-road study. The drivers on-road did not experience the roll motion as induced excitations but as road noise. This contradiction also has to do with the difference in how road unevenness

Table 4.4: *Properties of the predictive model from on-road with independent variables similar to that of driving simulator study*

	Frequency range [Hz]	β_k	p-value	I_k
offset		$6.13 \cdot 10^{-03}$ [-]	0.98	–
$\omega_{x,std}^{excess}$	0.25-0.5	-3.70 [s/deg]	$0.39 \cdot 10^{-07}$	0.11
	0.5-1	-10.23 [s/deg]	$0.51 \cdot 10^{-15}$	0.18
$\omega_{z,std}^{excess}$	0.5-1	26.95 [s/deg]	$0.38 \cdot 10^{-15}$	0.21
	1-2	11.46 [s/deg]	$0.48 \cdot 10^{-04}$	0.08
$\delta_{sw,std}$	1-2	10.39 [1/deg]	$0.12 \cdot 10^{-04}$	0.19
	2-4	-28.00 [1/deg]	$0.40 \cdot 10^{-08}$	0.22

act on the vehicle in the two studies, as previously discussed.

The model from on-road tests, Table 4.4, shows an increase in sensitivity for steering, δ_{sw}, frequency content at $1-2$ Hz which is opposite to that observed from the driving simulator study but the sensitivity is significantly reduced by the higher frequency range of $2-4$ Hz. The lateral acceleration, a_y, and steering, δ_{sw}, at $1-2$ Hz showed high correlation which implies from the model that steering at $1-2$ is either input or response by the driver that relates to observable self-induced or external excitations respectively. Nevertheless, since the higher frequency range of $2-4$ Hz has a higher impact on the model, the combined impact of the two frequency ranges is in line with the driving simulator model. The influence, I, of the combined steering frequency range $1-4$ Hz, is reduced from 0.16 to 0.12 when investigated between the model with direct variables and the model with excess motion variables. The details of these models are discussed in [61].

Table 4.5 shows the predictive model properties with the inclusion of all measured variables. Similar to the driving simulator study, the excess motion variables significantly reduced the influence of steering. The inclusion of the three additional measured variables with high significance (p-value < 0.001) in this predictive model improved the accuracy of the model to correctly predict the drivers' ability to identify an excitation from 67.7% to 71.7%. The standard deviation of absolute wind magnitude fluctuations, $v_{wind,mag,std}$, of frequency range $0.5-1$ Hz, is one of the included variables. The second variable is the standard deviation of absolute lateral acceleration felt by the drivers' upper body, $a_{y,head,std}$, at $1-2$ Hz. The $a_{y,std}^{excess}$ at $1-2$ Hz is found to be replaced by $a_{y,head,std}$. This finding suggests that the direct lateral acceleration felt by the drivers' upper body at $1-2$ Hz adds to the probability of observing external excitations. This is in line with the primary resonance of the upper body [66]. The model shows that the lateral acceleration together with yaw rotation (lateral motion) is present from $0.25-2$ Hz and roll motion between $0.25-1$ Hz. The negative β of $a_{x,std}$ suggests that the presence of vehicle longitudinal unsteady noises reduces the drivers' sensitivity to excitations but its impact is the least among the variables in this model.

Table 4.5: *Properties of the predictive model from on-road with the inclusion of all measured variables*

	Frequency range [Hz]	β_k	p-value	I_k
offset		-1.25 [-]	$0.11 \cdot 10^{-04}$	-
$a_{y,std}^{excess}$	0.25-0.5	15.90 [s^2/m]	$0.41 \cdot 10^{-06}$	0.07
$\omega_{x,std}^{excess}$	0.25-0.5	-5.16 [s/deg]	$0.49 \cdot 10^{-10}$	0.11
	0.5-1	-9.67 [s/deg]	$0.53 \cdot 10^{-12}$	0.13
$\omega_{z,std}^{excess}$	0.5-1	20.24 [s/deg]	$0.20 \cdot 10^{-08}$	0.12
$\delta_{sw,std}$	1-2	12.51 [1/deg]	$0.62 \cdot 10^{-07}$	0.17
	2-4	-29.88 [1/deg]	$0.10 \cdot 10^{-08}$	0.18
$a_{y,head,std}$	1-2	45.44 [s^2/m]	$0.22 \cdot 10^{-09}$	0.10
$v_{wind,mag,std}$	0.5-1	2.06 [s/m]	$0.14 \cdot 10^{-07}$	0.08
$a_{x,std}$	0.5-1	-38.17 [s^2/m]	$0.90 \cdot 10^{-04}$	0.05

Table 4.6: *Properties of the alternative predictive model from on-road with exclusion of direct involvement of steering*

	Frequency range [Hz]	β_k	p-value	I_k
offset		-1.19 [-]	$0.12 \cdot 10^{-06}$	-
$a_{y,std}^{excess}$	0.25-0.5	19.71 [s^2/m]	$0.11 \cdot 10^{-08}$	0.16
$a_{y,std}$	1-2	28.35 [s^2/m]	$0.88 \cdot 10^{-10}$	0.18
$\omega_{x,std}^{excess}$	0.25-0.5	-4.89 [s/deg]	$0.10 \cdot 10^{-09}$	0.21
	0.5-1	-9.24 [s/deg]	$0.27 \cdot 10^{-12}$	0.24
$\omega_{z,std}^{excess}$	0.5-1	18.29 [s/deg]	$0.24 \cdot 10^{-09}$	0.21

An alternative model was derived from direct and excess motion variables excluding steering, Table 4.6. The algorithm used for variables selection chose excess variables prior to their direct variables provided the respective p-value was not higher. The variables for selection represented vehicle rotational rates, lateral acceleration, and steering. In this model, the only excess motion variable replaced with direct variable is $a_{y,std}^{excess}$ at $1 - 2$ Hz. This model, with no high frequency steering noise as input, provides a better application in the early development phase of a vehicle design. A trend is observed in Tables 4.5 and 4.6 that signifies a straightforward relation between identifying excitations and the direct reading of lateral motion at $1 - 2$ Hz. The excess motion variables lie below 1 Hz, an indication that at least the effects of slow steering motion should be removed to improve the prediction of observable excitations.

In general, from on-road test a vehicle motion in the $0.5 - 1$ Hz range is most important for drivers experiencing excitations, followed by $0.25 - 0.5$ Hz and $1 - 2$ Hz. The predictive models from this study brought some insight into influential variables under controlled test environment in driving simulator and under on-road conditions. The model identified the significance of road induced roll noise causing lower sensitivity of the drivers. This supports the observation from the study by Nguyen et al. [38]. The frequency ranges of the variables that most influence the drivers' sensitivity to any induced excitation are observed from the predictive model. The models also confirmed the trend of the influence of steering and yaw velocity on driver sensitivity under both test conditions.

4.4   Proposed transfer function using dynamic model

The transfer function approach is proposed to obtain the excess motion variables which correlate better with the influence of external disturbances, such as aerodynamic excitations, and enhance the predictive model. The approach utilizes the weighted transfer function, $\bar{H}_{\delta_{sw} \to \omega_i^{steer}}$ or $\bar{H}_{\delta_{sw} \to a_y^{steer}}$. The dynamic model discussed in Section 3.1.4 was used to analyze the proposed transfer function. As a case study, a yaw moment disturbance, M_z, Equation 3.20, was fed to the vehicle model A as shown in Figure 3.3. The yaw moment disturbance is introduced 5 seconds after the start of the simulation, shown in Figure 4.10.
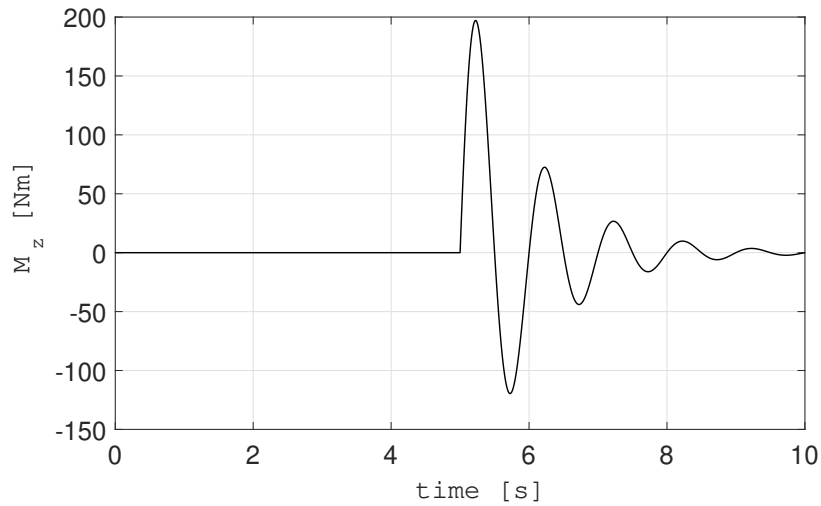
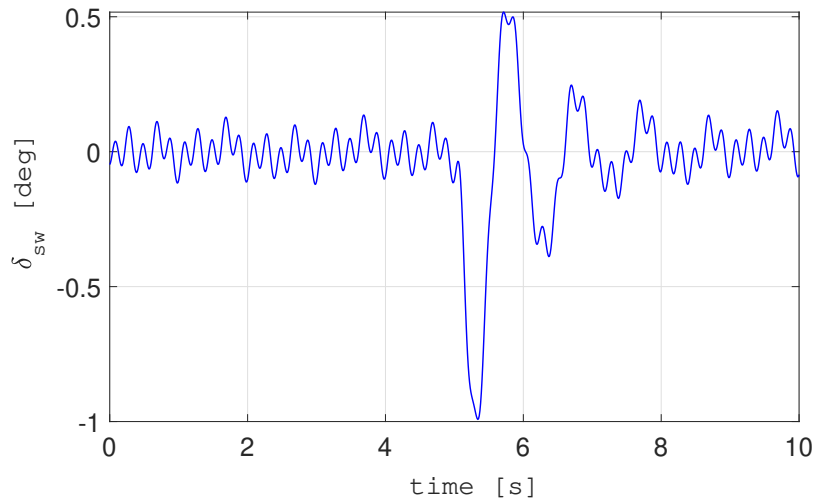**Figure 4.10:** *Yaw moment disturbance M_z fed to the vehicle model A*

Figure 4.11: *Driver's steering, δ_{sw}, over the simulated time from the driver/driver model.*

Figure 4.11 shows the driver's steering over the simulated time. The noise added in the equation of the driver model, Equation 3.21, is seen throughout the simulation time. Figure 4.12 shows the resulting the direct yaw velocity, ω_z, yaw velocity due to steering, ω_z^{steer}, excess yaw velocity from simulation, ω_z^{excess}(simulated), and excess yaw velocity estimated from proposed transfer function approach, ω_z^{excess}(estimated). From the dynamic model, the absolute value of ω_z^{excess} obtained by running the model and estimated from implementing the proposed transfer function approach with the input variables from the model were compared, Figure 4.13. Both ω_z^{excess} showed a similar trend with comparable amplitudes but the proposed approach contains small background noise. The weighted transfer function, $\bar{H}_{\delta_{sw} \to \omega_z^{steer}}$, is composed of data with discrete frequencies and respective gain values which explains the presence of noise. Optimizing the process of obtaining the transfer function will help to reduce the noise level. The profile of ω_z^{excess} shown in Figure 4.12 is identical to a yaw moment disturbance, M_z, shown in Figure 4.10. The estimated ω_z^{excess} from the proposed approach also showed the same profile but with background noise, Figure 4.13. The analysis supports the application of the weighted transfer function approach to estimate the excess motion variables that correlate well with
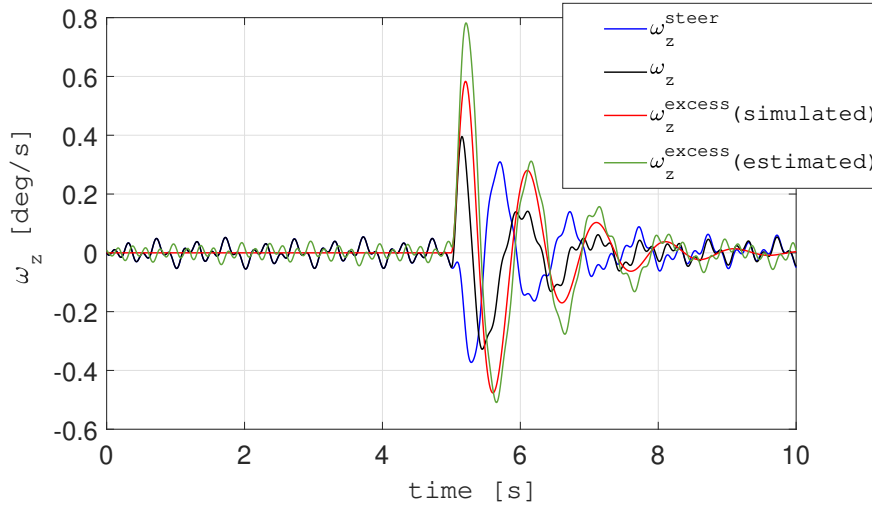
Figure 4.12: *Output variables direct yaw velocity, ω_z, yaw velocity due to steering, ω_z^{steer}, and excess yaw velocity, ω_z^{excess} (simulated), and ω_z^{excess} (estimated), from both methods.*
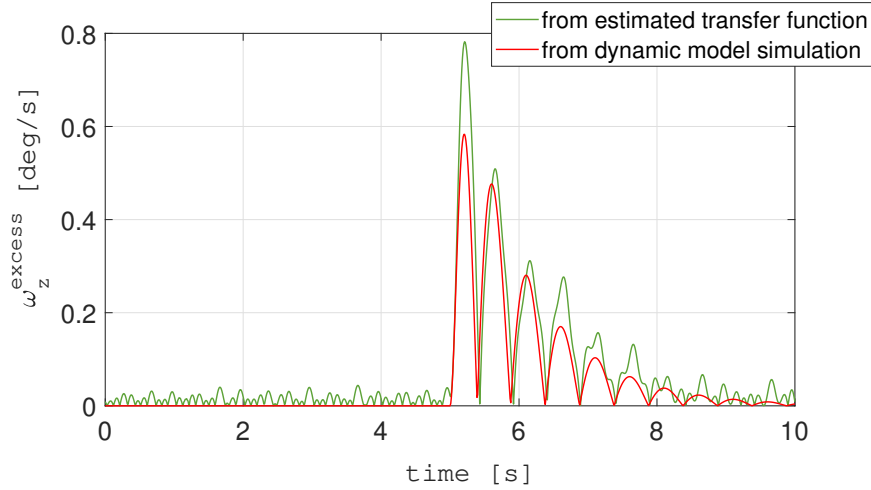

Figure 4.13: *Comparison of the absolute value of ω_z^{excess} obtained by running the dynamic model and ω_z^{excess} estimated from weighted transfer function, $\bar{H}_{\delta_{sw} \to \omega_z^{steer}}$ approach over the input variables from the dynamic model.*

the external disturbance. The analysis was done by building a transfer function from ω_z^{steer} and δ_{sw}. Replacing the ω_z^{steer} with ω_z as done for this thesis resulted in the same pattern of the absolute value of ω_z^{excess} between the two methods as mentioned above but with higher noise background. An increase in sample size showed a significant improvement in the absolute value of ω_z^{excess} correlation between the two methods and a reduction in the noise.

This section confirms that the signal processing using transfer function works and also shows how a conceptional time domain vehicle dynamics model can be used as alternative way to create the excess signals. The weighted transfer function of steering to relevant motions such as $\bar{H}_{\delta_{sw} \to \omega_i^{steer}}$ and $\bar{H}_{\delta_{sw} \to a_y^{steer}}$ of a vehicle prototype can be received from the engineers. This is a fast and simple approach to obtain excess motion variables without the need of any other vehicle parameters.

4.5   Implementation of proposed predictive model

The proposed predictive model can be used to study the perceived vehicle stability of a given vehicle. Figure 4.14 shows the layout of a possible implementation of the model that predicts the occurrence of observable aerodynamic excitations.

The estimated excess motion variables can be obtained from the transfer function approach or a dynamic model. The predictive model can be applied for both early and later phase of vehicle development. In the former application, the layout will evaluate perceived vehicle stability at high speed in early stages of development before any drivable real vehicle prototype is available.

4.5.1   For early development phase

Early phase of vehicle development includes simulations such as wind tunnel tests, computational fluid dynamics (CFD), and vehicle dynamic simulations. For predicting the occurrence of observable aerodynamic excitations involving these simulations, the choice of the predictive model is wider. The predictive model with properties shown in Table 4.3 is suitable for investigating the observable excitations on a vehicle model using vehicle dynamic simulations with a focus on axis component force or moment fluctuations. The influence of other external disturbances such as road unevenness is minimal in the model.

The predictive model with properties shown in Table 4.6 contains the influence of road unevenness and more realistic coupled aerodynamic excitations' forces and moments experienced on-road. This model does not consider the direct impact of high steering noise in predicting observable excitations. For the simulated tests, the direct variables are computed quantities that represent aerodynamic properties, steering, and vehicle motion. This predictive model shows the variables of significance and their respective frequency ranges. As described in the previous section, the excess motion variables can be obtained from the direct variables and the
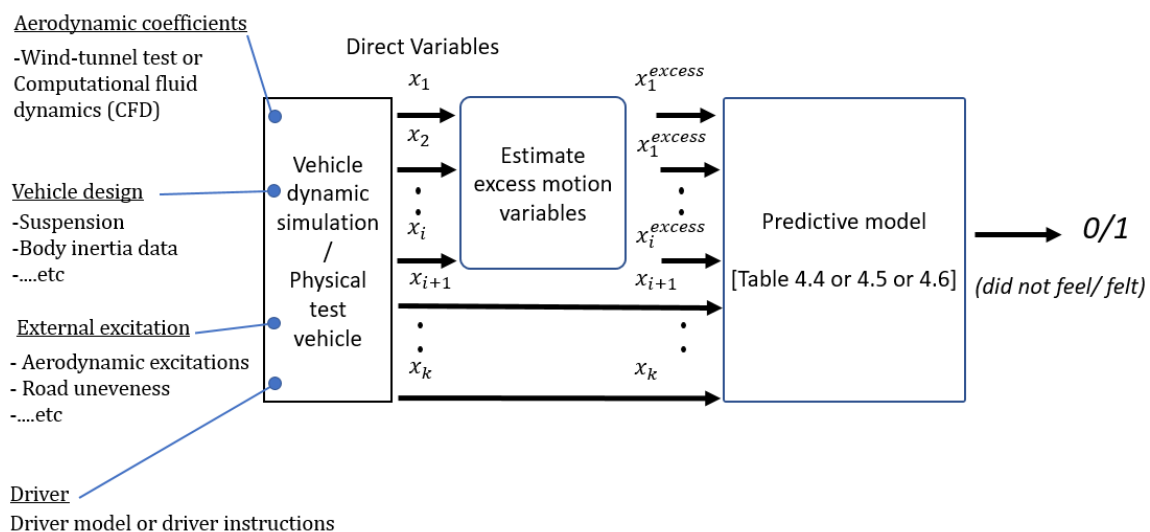

Figure 4.14: *Layout of a possible implementation of the predictive model.*

weighted transfer function approach or the dynamic model. The weighted transfer function can be calculated from the vehicle dynamic of the prototype model. These two predictive models, represented by the model properties Tables 4.3 and 4.6, are relevant for early development studies of vehicle design and perceived stability.

Table 4.5 represents properties of the predictive model from the on-road tests where the influence of the absolute wind magnitude fluctuation and reduced sensitivity from road induced roll and longitudinal motions are present. This model is also suitable for further investigating the perceived stability under wind and longitudinal force fluctuations during early phase of development.

The predictive models from the on-road study, model properties shown by Tables 4.5 and 4.6, represent only professional test drivers' perceived stability.

4.5.2 For later development phase

Tests of physical pre-production vehicles on-road can only be done during the later development phase and by professional test drivers. In this case, the properties of the predictive model shown in Table 4.5 are suitable for perceived vehicle stability on-road. The model includes lateral accelerations felt at the headrest and external disturbances and related measured variables such as absolute headwind magnitude. Similar to previous models, the excess motion variables can be calculated from direct variables using the weighted transfer function approach or the dynamic model. Only the variables shown in Table 4.5 filtered to their frequency ranges of significance are needed to estimate the occurrence of observable aerodynamic excitations.

5

Conclusions

The findings in this study provide insight into the relationship between subjective evaluation of drivers and measurable quantities on vehicle behavior during straight-line high speed driving, under external excitations such as unsteady aerodynamics. The outcomes of this study can be used to improve early phase development prediction of aerodynamic vehicle stability when no drivable physical vehicle prototype is available.

The initial on-road experiment was aimed at finding a relation between the subjective evaluation of perceived stability and measurable quantities such as steering responses, and linear and rotational motions. Several aerodynamic devices were used to excite varying forces and moments: An inverted wing, an inverted wing with fin, and an anti-diffuser. These were paired with and without sidekicks. The paired comparisons showed that the presence of side-kicks improved perceived straight-line stability. Two methods to visualize the overall average subjective evaluation between devices with measured variables were presented. The vector plots of mean and standard deviation pointed toward the origin (when plotting pairs from without sidekick to with sidekick) implying that the vehicle response and steering effort to aerodynamic excitations were reduced with side-kicks, thus increasing perceived stability. The ride diagram helped to differentiate the influence of transient and stationary behaviour. The devices were able to reduce nervous vehicle behaviour without changing the rear lift coefficient or front-rear lift distribution.

The experiments from driving simulators and on-road tests focused on obtaining data for regression models to predict which excitations drivers can feel in relation to objective quantities. The model from the driving simulator test quantified the difference in sensitivity between driver types (common drivers and test drivers) and the difference in sensitivity to yaw and roll excitations. Compared to common drivers, professional test drivers were more sensitive to yaw moment excitations at all tested frequency ranges but not roll moment excitations. The impact of steering at $1 - 2$ Hz affects the drivers' sensitivity to externally induced excitations. Professional test drivers steered less than common drivers. This partially explains the higher sensitivity of test drivers. The on-road predictive model shows that vehicle motion at $0.5 - 1$ Hz range is most important for drivers experiencing excitations. Similar to the model from the driving simulator, higher frequency steering, at $1 - 4$ Hz, affects the drivers' sensitivity to externally induced excitations. The on-road noise results in higher rolling and longitudinal motions that reduced the drivers' sensitivity to external excitations. The absolute lateral motion of drivers' upperbody at $1 - 2$ Hz and the absolute wind magnitude fluctuations around $0.5 - 1$ Hz contribute to the drivers' identification of excitations. Both tests support that drivers

are more sensitive to yaw excitations than roll. A layout is proposed for the implementation of the predictive model for both on-road test and simulations.

The results obtained from the on-road and driver simulator tests provide an opportunity for assessing and investigating flow characteristics that could result in excitations in the form of vehicle instabilities for the driver.

Concluding the thesis findings by reviewing the thesis objective:

- *For high speed straight-line driving under aerodynamic excitations, how can objective quantities such as steering response, and linear and rotational accelerations be related to the subjective evaluation of drivers?*

  From the test results, it was shown that the relative subjective evaluation of drivers' within paired configurations can be visually represented with objective quantities using vector plots and ride diagrams. Furthermore, the developed predictive models also relate subjective evaluation of the drivers to objective quantities.

- *Is it possible to predict a driver's ability to identify an induced disturbance in an early vehicle design phase?*

  Yes, the derived predictive models can be used to pinpoint the occurrence time of observable aerodynamic excitations in an early vehicle design phase. The models provide a base for filtering aerodynamic excitations or fluctuations in terms of frequencies and amplitudes. They can also be used to identify which signals and frequency ranges can be ignored when searching for problematic excitations.

- *How can a predictive model be used to identify instabilities before any drivable vehicle prototype is available?*

  For this application, a layout for the implementation of the predictive model is proposed in Section 4.5. It provides a platform for simulation tools that help identifying perceived instabilities in the early design phase.

6

Future work

In the case of driving simulator trials, more data collection should be carried out with a greater and better-adjusted range in amplitude. Likewise, studying yaw and lateral motion separately, and more complex disturbance combinations are of interest. The impact of road noises on the driving simulator which is more relatable to on-road conditions should be further investigated. Further collection of data with more participants with different aerodynamic designs with generalized vehicle dynamic properties such as tires would help in building more generic predictive models. The use of different vehicle dynamic properties can further investigate the influences of different variables. More work is needed to decide how well the proposed implementation of predictive model antecipates the observable excitations.

The study on steering behaviour and the involvement of driver interaction create uncertainties. As a result, an in-depth study relating to noises created by driver-vehicle interactions will add further understanding of vehicle stability.

A study to verify the predictive model using wind tunnel tests and CFD simulations on a generic or specific vehicle prone to aerodynamic instabilities will be beneficial. The wind tunnel balance should be able to record time-resolved measurements with high resolutions in order to capture the aerodynamic excitation characteristics. Additionally, measuring surface pressures around the aerodynamically stable and unstable configurations when driving on road would be desirable. Of course, the same is valid with CFD or wind tunnel tests in order to draw conclusions from the data. The research could also be extended to more complex cases like cornering, bumpy roads and braking or combinations of those.

7

Summary of papers

7.1 Paper A

Analysis of Subjective Qualitative Judgement of Passenger Vehicle High Speed Drivability due to Aerodynamics

This paper focuses on finding a relationship between the vehicle motion and subjective evaluation of high-speed straight-line perceived stability. The test was performed on a front-load biased compact sedan at the Volvo Cars Hällered Proving Ground. Different aerodynamic devices were used for generating higher lift and asymmetric aerodynamic forces resulting in substandard straight-line perceived stability on-road. The resulting poor perceived stability of the test vehicle with the aerodynamic devices was improved with the help of side-kicks. The paper investigates the trend of perceived stability of configurations with and without side-kicks in relation to vector plots of mean and standard deviation. The ride diagram was used to separate the presence of transient behaviour and study its impact on subjective evaluation. The qualitative assessment of the resulting trends agrees well with the subjective evaluation of the driver.

7.2 Paper B

Prediction of Driver's Subjective Perception and Vehicle Reaction under Aerodynamic Excitations

This paper investigates drivers' subjective evaluation and responses to aerodynamic excitations in high-speed straight-line driving condition. Clinical tests involving both common and professional test drivers were conducted using driving simulators at Volvo Cars and VTI. The results provided insight into the disturbance frequencies and amplitudes of interest. The paper presents a model from the test data that can predict the drivers' subjective evaluation after experiencing induced aerodynamic excitations. The drivers were more sensitive to yaw excitations than roll excitations. The impact of drivers' steering actions on their subjective evaluations of these excitations is also shown.

7.3   Paper C

Improved Prediction Model of Drivers' Subjective Perception of Vehicle Reaction under Aerodynamic Excitations

The driving simulator study in Paper B was extended with a deeper analysis. The accuracy of the model was improved by doubling the sample sizes, replacing directly measured variables with excess variables and by splitting measured variables into frequency ranges using bandpass filtering. Excess motion variables are defined as the part of vehicle motion that is not the direct result of steering action. Moreover, excess motion variables reduce the importance of steering as a separate variable in the predictive model. Paper B showed that the drivers were more sensitive to yaw excitations than roll excitations. The updated model shows that the drivers' sensitivity to roll velocity in the frequency range 0.25-0.5 Hz is comparable to yaw velocity. The impact of drivers' steering on their subjective evaluations of these excitations is significant only around to 1-2 Hz. The study also reveals the crucial frequency range of other measured variables that influence the updated predictive model.

7.4   Paper D

Predictive Model of Driver's Perception of Vehicle Stability under Aerodynamic Excitation

Paper B and paper C are extended by collecting on-road data and using that instead of driving simulator data to fit predictive models. The similarities and differences between the models are compared with those from Paper C. The study shows that the reduced importance of steering and the improvement in accuracy of the predictive model with the help of excess motion variables found in the driving simulator is also valid in on-road conditions. Similar to the findings in Paper C, the reduction of drivers' sensitivity to aerodynamic excitations due to steering is significant around 1-4 Hz. The models show the drivers to be more sensitive to yaw motion than roll motion. Roll motion lower the drivers' sensitivity to excitations, which is in contradiction to the findings in Paper C. The reason may be the presence of realistic and higher amplitude on-road noise transfer. The study suggests that the drivers experience the excitations the most with the resulting vehicle motion in the 0.5-1 Hz range, followed by 0.25-0.5 Hz and 1-2 Hz. In addition, the absolute lateral acceleration felt by the drivers' upper body, at 1-2 Hz and absolute wind magnitude fluctuations at 0.5-1 Hz contribute to the drivers' ability to identify excitations.

References

[1] Hucho, W. H. "Aerodynamics of Road Vehicles". *SAE International* (1998).

[2] Brandt, A. "Unsteady aerodynamic effects on the driving stability of passenger vehicles". *PhD thesis, Department of Mechanics and Maritime Sciences Chalmers University of Technology* (2023).

[3] Favre, T., Näfver, J. J., Jerrelind, J., Trigell, A. S., and Efraimsson, G. "Static coupling between detached-eddy simulations and vehicle dynamic simulations of a generic road vehicle model with different rear configurations in unsteady crosswind". *International Journal of Vehicle Design* **72**.4 (2016). DOI: 10.1504/ijvd.2016.082384.

[4] Nakashima, T., Tsubokura, M., Ikenaga, T., and Doi, Y. "HPC-LES for Unsteady Aerodynamics of a Heavy Duty Truck in Wind Gust - 2nd report: Coupled Analysis with Vehicle Motion". *SAE Technical Paper Series* (2010). DOI: 10.4271/2010-01-1021.

[5] Lewington, N., Ohra-aho, L., Lange, O., and Rudnik, K. "The Application of a One-Way Coupled Aerodynamic and Multi-Body Dynamics Simulation Process to Predict Vehicle Response during a Severe Crosswind Event". *SAE Technical Paper Series* (2017). DOI: 10.4271/2017-01-1515.

[6] Kee, J. D., Rho, J. H., Kim, K. H., and Lee, D. H. "High speed driving stability of passenger car under crosswind effects". *International Journal of Automotive Technology* **15**.5 (2014), 741–747. DOI: 10.1007/s12239-014-0077-8.

[7] Bell, J. R., Wilhelmi, H., Heine, D., Jessing, C., Wagner, A., Wiedemann, J., Ehrenfried, K., and Wagner, C. "Experimental Investigation of Automotive Vehicle Transient Aerodynamics with a Reduced-Scale Moving-Model Crosswind Facility". *SAE Technical Paper Series* (2020). DOI: 10.4271/2020-01-0671.

[8] Bell, J. R., Wilhelmi, H., Heine, D., Jessing, C., Wagner, A., Wiedemann, J., and Wagner, C. "Aerodynamic Characterization of a Full-Scale Compact Car Exposed to Transient Crosswind". *SAE International Journal of Passenger Cars - Mechanical Systems* **14**.1 (2021), 06-14-01–0001. DOI: 10.4271/06-14-01-0001.

[9] Carbonne, L., Winkler, N., and Efraimsson, G. "Use of Full Coupling of Aerodynamics and Vehicle Dynamics for Numerical Simulation of the Crosswind Stability of Ground Vehicles". *SAE International Journal of Commercial Vehicles* **9**.2 (2016), 359–370. DOI: 10.4271/2016-01-8148.

[10] Forbes, D., Page, G., Passmore, M., and Gaylard, A. "A Fully Coupled, 6 Degree-of-Freedom, Aerodynamic and Vehicle Handling Crosswind Simulation using the DrivAer Model". *SAE International Journal of Passenger Cars - Mechanical Systems* **9**.2 (2016). DOI: 10.4271/2016-01-1601.

[11] Nakashima, T., Tsubokura, M., Vázquez, M., Owen, H., and Doia, Y. "Coupled analysis of unsteady aerodynamics and vehicle motion of a road vehicle in windy conditions". *Computers & Fluids* **80** (2013), 1–7. DOI: 10.1016/j.compfluid.2012.09.028.

[12] Klasson, J. "A Generalised Crosswind Model for Vehicle Simulation Purposes". *Vehicle System Dynamics* **37** (2002), 827–835. DOI: 10.1080/00423114.2002.11666245.

[13] Juhlin, M. "Aerodynamic loads on buses due to crosswind gusts – on-road measurements". *Vehicle System Dynamics* **46** (2008), 350–359. DOI: 10.1080/00423110802037081.

[14] Nakasato, K., Tsubokura, M., Ikeda, J., Onishi, K., and al, et. "Coupled 6 DoF Motion and Aerodynamic Crosswind Simulation Incorporating Driver Model". *SAE International Journal of Passenger Cars - Mechanical Systems* **10**.2 (2017), 662–670. DOI: `10.4271/2017-01-1525`.

[15] Schroeck, D., Krantz, W., Widdecke, N., and Wiedemann, J. "Unsteady Aerodynamic Properties of a Vehicle Model and their Effect on Driver and Vehicle under Side Wind Conditions". *SAE International Journal of Passenger Cars - Mechanical Systems* **4**.1 (2016), 108–119. DOI: `10.4271/2011-01-0154`.

[16] Baker, C. J. and Reynolds, S. "Wind-induced accidents of road vehicles". *Accident Analysis & Prevention* **24**.6 (1992), 559–575. DOI: `10.1016/0001-4575(92)90009-8`.

[17] Macadam, C. C., Sayers, M. W., Pointer, J. D., and Gleason, M. "Crosswind Sensitivity of Passenger Cars and the Influence of Chassis and Aerodynamic Properties on Driver Preferences". *Vehicle System Dynamics* **19**.4 (1990), 201–236. DOI: `10.1080/00423119008968942`.

[18] Howell, J. and Panigrahi, S. "Aerodynamic Side Forces on Passenger Cars at Yaw". *SAE World Congress and Exhibition* (2016). DOI: `10.4271/2016-01-1620`.

[19] Theissen, P. "Unsteady Vehicle Aerodynamics in Gusty Crosswind". *PhD thesis, Technical University of Munich* (2012). URL: `http://mediatum.ub.tum.de/doc/1096026/520174.pdf`.

[20] Willumeit, H. P., Müller, K., Dödlbacher, G., and Matheis, A. "Method to correlate vehicular behaviour and driver's judgment under side wind disturbance". *Vehicle System Dynamics* **17** (1988), 508–524. DOI: `10.1080/00423118808969292`.

[21] Kawamura, T. and Ogawa, A. "Effect of Unsteady Lift Force on Vehicle Dynamics in Heave and Pitch Motion". *SAE Technical Paper Series* **8**.1 (2014), 205–216. DOI: `10.4271/2014-01-0576`.

[22] Okada, Y., Nouzawa, T., Nakamura, T., and Okamoto, S. "Flow Structures above the Trunk Deck of Sedan-Type Vehicles and Their Influence on High-Speed Vehicle Stability 1st Report: On-Road and Wind-Tunnel Studies on Unsteady Flow Characteristics that Stabilize Vehicle Behavior". *SAE International Journal of Passenger Cars - Mechanical Systems* (2009), 138–156. DOI: `10.4271/2009-01-0004`.

[23] Nakashima, T., Tsubokura, M., Nouzawa, T., and Nakamura, T. "Flow Structures above the Trunk Deck of Sedan-Type Vehicles and Their Influence on High-Speed Vehicle Stability 2nd Report: Numerical Investigation on Simplified Vehicle Models using Large-Eddy Simulation". *SAE International Journal of Passenger Cars - Mechanical Systems* (2009), 157–167. DOI: `10.4271/2009-01-0006`.

[24] Kawakami, M., Murata, O., and Maeda, K. "Improvement in Vehicle Motion Performance by Suppression of Aerodynamic Load Fluctuations". *SAE International Journal of Passenger Cars - Mechanical Systems* **8**.1 (2015), 205–216. DOI: `10.4271/2015-01-1537`.

[25] Howell, J. and Le Good, G. "The Influence of Aerodynamic Lift on High Speed Stability". *SAE International* **8**.8 (1999). DOI: `10.4271/1999-01-0651`.

[26] Buchheim, R., Maretzke, J., and Piatek, R. "The Control of Aerodynamic Parameters Influencing Vehicle Dynamics". *SAE Paper, 850279–850279* (1985). DOI: `10.4271/850279`.

[27] Kim, D., Jeong, M., Bae, B., and Ahn, C. "Design of a Human Evaluator Model for the Ride Comfort of Vehicle on a Speed Bump Using a Neural Artistic Style Extraction". *Sensors* **19**.24 (2019). DOI: `10.3390/s19245407`.

[28] Wang, Y., Zhang, Q., Zhang, L., and Hu, Y. "A Method to Automatic Measuring Riding Comfort of Autonomous Vehicles: Based on Passenger Subjective Rating and Vehicle Parameters". *Conference: Design, User Experience, and Usability. Application Domains. Springer International Publishing* (2019), 130–145. DOI: `10.1007/978-3-030-23538-3_10`.

[29] Apfelbeck, A., Henze, R., and Kücükay, F. "Unsteady Aerodynamic Properties of a Vehicle Model and their Effect on Driver and Vehicle under Side Wind Conditions". *SAE International Journal of Vehicle Dynamics, Stability, and NVH* **5**.2 (2021), 113–129. DOI: `10.4271/10-05-02-0008`.

[30] Heiderich, M., Friedrich, T., and Nguyen, M. T. "New approach for improvement of vehicle performance by using a simulation-based optimization and evaluation method". 7th *International Munich Chassis Symposium, ATZ, Munich* (2016). DOI: `https://10.1007/978-3-658-14219-3-21`.

[31] Fainello, M., Ferrari SpA-Diego Minen, and VI-grade. "Active vehicle ride and handling development by using integrated SIL / HIL techniques in a high performance driving simulator". *5th International Munich Chassis Symposium* (2014). DOI: `10.1007/978-3-658-14219-321`.

[32] Stewart, D. "A Platform with Six Degrees of Freedom". *Proceedings of the Institution of Mechanical Engineers* **180** (1965), 371–386.

[33] Kuschov, A. "Motion Perception and Tire Models for Winter Conditions in Driving Simulators". *Licentiate thesis, Department of Mechanics and Maritime Sciences Chalmers University of Technology* (2016).

[34] VTI. "Driving simulator facilities" (). URL: `https://www.vti.se/en/research/vehicle-technology-and-driving-simulation/driving-simulation/simulator-facilities`. accessed on 20 April 2021.

[35] Blissing, B., Bruzelius, F., and Eriksson, O. "Effects of Visual Latency on Vehicle Driving Behavior". *ACM Transactions on Applied Perception* **14**.1 (2016), 1–12. DOI: `10.1145/2971320`.

[36] Krantz, W., Pitz, J. O., Stoll, D., and Nguyen, M. T. "Simulation des Fahrens unter instationärem Seitenwind". *Automobiltechnische Zeitschrift* **116** (2014), 64–68. DOI: `10.1007/s35148-014-0046-6`.

[37] Huemer, J., Stickel, T., Sagan, E., Schwarz, M., and Wolfgang, A. W. "Influence of unsteady aerodynamics on driving dynamics of passenger cars". *Vehicle System Dynamics* **52**.11 (2015), 1470–1488. DOI: `10.1080/00423114.2014.944191`.

[38] Nguyen, M., Pitz, J., Krantz, W., Neubeck, J., and Wiedemann, J. "Subjective Perception and Evaluation of Driving Dynamics in the Virtual Test Drive". *SAE International Journal of Vehicle Dynamics, Stability, and NVH* **1**.2 (2017), 247–252. DOI: `10.1080/00423114.2014.944191`.

[39] Fuller, J., Best, M., Garret, N., and Passmore, M. "The importance of unsteady aerodynamics to road vehicle dynamics". *Journal of Wind Engineering and Industrial Aerodynamics* **117** (2013), 1–10. DOI: `10.1016/j.jweia.2013.03.006`.

[40] Benson, A. J., Spencer, M. B., and Stott, J. R. "Thresholds for the detection of the direction of whole-body, linear movement in the horizontal plane". *Aviation, space, and environmental medicine* (1986).

[41] Groen, E. and Bles, W. "How to use body tilt for the simulation of linear self motion". *Journal of Vestibular Research* **14**.5 (2004), 375–385.

[42]   Mesland, B., Bles, W., Wertheim, A., and Groen, E. "The influence of expectation on the perception of linear horizontal motion". *TNO Human Factors Research Institute, Soesterberg, The Netherlands,* (1998). DOI: `ReportTM-98-A010`.

[43]   Wagner, A. and Wiedemann, J. "Crosswind Behavior in the Driver's Perspective". *World Congress & Exhibition. SAE International* (2002). DOI: `10.4271/2002-01-0086`.

[44]   Strandemar, K. and Thorvald, B. "Truck Characterizing Through Ride Diagram: In Vehicle Dynamics and Chassis Developments". *SAE Commercial Vehicle Engineering Congress* (2004), 913–920. DOI: `10.4271/2004-01-2714`.

[45]   Strandemar, K. and Thorvald, B. "Driver perception sensitivity to changes in vehicle behavior". *Vehicle System Dynamics* (2004), 272–281.

[46]   Strandemar, K. "An Objective Measures for Ride Comfort Evaluation". *Ph.D. Thesis, Control Technology, Stockholm, Sweden* (2005).

[47]   Strandemar, K. and Thorvald, B. "The Ride Diagram, A Tool for Analysis of Vehicle Suspension Settings: The Dynamics of Vehicles on Roads and on Tracks". *Vehicle System Dynamics International Journal of Vehicle Mechanics and Mobility* **44** (2006), 913–920. DOI: `10.1080/00423110600907618`.

[48]   Williamson, A. M., Feyer, A. M., and Friswell, R. "The impact of work practices on fatigue in long distance truck drivers". *Accident Analysis and Prevention* **26**.28 (1996), 709–719. DOI: `0.1016/s0001-4575(96)00044-9`.

[49]   Lal, S. K. L. and Craig, A. "A critical review of the psychophysiology of driver fatigue". *Biological Psychology* **55**.3 (2001), 173–194. DOI: `10.1016/s0001-4575(02)00014-3`.

[50]   Thiffault, P. and Bergeron, J. "Monotony of road environment and driver fatigue: A simulator study". *Accident Analysis and Prevention* **35**.6 (2003), 381–391. DOI: `10.1016/s0001-4575(02)00014-3`.

[51]   Ranney, T. A., Simmons, L. A., and Masalonis, A. J. "Prolonged exposure to glare and driving time: Effects on performance in a driving simulator". *Accident Analysis and Prevention* **31**.6 (1999), 601–610. DOI: `10.1016/s0001-4575(99)00016-0`.

[52]   Kecklund, G. and Åkerstedt, T. "Sleepiness in long distance truck driving: An ambulatory EEG study of night driving". *Ergonomics* **12**.36 (1993), 1007–1017. DOI: `10.1080/00140139308967973`.

[53]   Hamilton, J. D. "Time Series Analysis". *Princeton University Press: Princeton, USA* **4** (2013).

[54]   Box, G. E. P., Jenkins, G. M., and Reinsel, G. C. "Time Series Analysis: Forecasting and Control". *John Wiley & Sons, New Jersey, US* **3** (2008).

[55]   Walker, S. H. and Duncan, D. B. "Estimation of the probability of an event as a function of several independent variables". *Princeton University Press: Princeton, USA* **54** (1967), 167–178. DOI: `10.2307/2333860`.

[56]   David, A. F. "Statistical Models: Theory and Practice". *Cambridge University Press* (2009), 128.

[57]   Sternéus, J., Walker, T., and Bender, T. "Upgrade of the Volvo Cars Aerodynamic Wind Tunnel". *Journal of Passenger Cars: Mechanical Systems Journal* **116**.6 (2007), 1089–1099. DOI: `10.4271/2007-01-1043`.

[58]   VI-Grade. "Documentation on VI-CarRealTime". URL: `https://www.vi-grade.com/en/products/vi-carrealtime.`. (accessed on 20 April 2021).

[59] Bruzelius, F., Gomez, F. J., and Augusto, B. "A Basic Vehicle Dynamics Model for Driving Simulators". *International Journal of Vehicle Systems Modelling and Testing* **8**.4 (2013), 364–385. DOI: 10.1080/00423114.2019.1566555.

[60] Obialero, E. "A Refined Vehicle Dynamic Model for Driving Simulators". *Master's Thesis. Chalmers University of Technology* (2013).

[61] Kumar, A., Sällström, E., Sebben, S., and Jacobson, B. "Predictive Model of Driver's Perception of Vehicle Stability under Aerodynamic Excitation". *SAE Technical Paper Series* (2023). DOI: 10.4271/2023-01-0903.

[62] Intrumentation, P. "Documentation". 2017. URL: %7B%20https://pm-instrumentation.com/docpdf/Systemes/embarque-volant/PMI-01184-Volant-telemetrique.pdf%7D. (accessed on 15 May 2019).

[63] Oettle, N. R., Sims-Williams, D., Dominy, R., Darlington, C., Freeman, C., and Tindall, P. "The Effects of Unsteady On-Road Flow Conditions on Cabin Noise". *SAE International Journal of Passenger Cars - Mechanical Systems* **4** (2011), 120–130. DOI: 10.4271/2011-01-0159.

[64] DEWESoft. "Documentation on IMU and GPS". 2019. URL: https://dewesoft.com/products/interfaces-and-sensors/gps-and-imu-devices. (accessed on 20 May 2021).

[65] Brandt, A., Jacobson, B., and Sebben, S. "High speed driving stability of road vehicles under crosswinds: an aerodynamic and vehicle dynamic parametric sensitivity analysis". *Vehicle System Dynamics* **60**.7 (2021), 2334–2357. DOI: 10.1080/00423114.2021.1903516.

[66] Lin, Z., Zhang, J., Li, J., Yin, W., Liu, C., and Lin, J. "Response of Seated Human Body to Roll Vibration and Correlation between Roll and Lateral Directions". *Shock and Vibration* **3** (2020), 1–12. DOI: 10.1155/2020/8839363.

[67] Kumar, A., Sebben, S., Sällström, E., Jacobson, B. J. H., and Broniewicz, A. "Analysis of Subjective Qualitative Judgement of Passenger Vehicle High Speed Drivability due to Aerodynamics". *Energies* **12**.14 (2019). DOI: 10.3390/en12142839.

[68] Kumar, A., Sällström, E., Sebben, S., Amiri, K., and Jacobson, B. "Prediction of Driver's Subjective Perception and Vehicle Reaction under Aerodynamic Excitations". *Human Factors* (2023). DOI: 10.1177/00187208231157935.

[69] Kumar, A., Sällström, E., Sebben, S., and Jacobson, B. "Improved Prediction Model of Drivers' Subjective Perception of Vehicle Reaction under Aerodynamic Excitations". *To be submitted* (2023).